



LAWRENCE  
LIVERMORE  
NATIONAL  
LABORATORY

# Myocyte Turnover in the Aging Human Heart

J. Kajstura, N. Gurusamy, B. Ogorek, C. C. Rondon, T. Hosoda, D. DAmario, S. Bardelli, A. P. Beltrami, D. Cesselli, R. Bussani, F. del Monte, F. Quaini, M. Rota, K. Urbanek, C. A. Beltrami, B. A. Buchholz, A. Leri, P. Anversa

September 8, 2010

Circulation Research

## **Disclaimer**

---

This document was prepared as an account of work sponsored by an agency of the United States government. Neither the United States government nor Lawrence Livermore National Security, LLC, nor any of their employees makes any warranty, expressed or implied, or assumes any legal liability or responsibility for the accuracy, completeness, or usefulness of any information, apparatus, product, or process disclosed, or represents that its use would not infringe privately owned rights. Reference herein to any specific commercial product, process, or service by trade name, trademark, manufacturer, or otherwise does not necessarily constitute or imply its endorsement, recommendation, or favoring by the United States government or Lawrence Livermore National Security, LLC. The views and opinions of authors expressed herein do not necessarily state or reflect those of the United States government or Lawrence Livermore National Security, LLC, and shall not be used for advertising or product endorsement purposes.

## Myocyte Turnover in the Aging Human Heart

Kajstura: Age, Gender and Cardiomyogenesis

<sup>1</sup>Jan Kajstura, <sup>1</sup>Narasimman Gurusamy, <sup>1</sup>Barbara Ogórek, <sup>1</sup>Carlos Clavo Rondon, <sup>1</sup>Toru Hosoda, <sup>1</sup>Domenico D'Amario, <sup>1</sup>Silvana Bardelli, <sup>2</sup>Antonio Paolo Beltrami, <sup>2</sup>Daniela Cesselli, <sup>3</sup>Rossana Bussani, <sup>4</sup>Federica del Monte, <sup>1</sup>Federico Quaini, <sup>1</sup>Marcello Rota, <sup>1</sup>Konrad Urbanek, <sup>2</sup>Carlo A. Beltrami, <sup>5</sup>Bruce A. Buchholz, <sup>1</sup>Annarosa Leri, <sup>1</sup>Piero Anversa

<sup>1</sup>Departments of Anesthesia and Medicine, and Cardiovascular Division, Brigham and Women's Hospital, Harvard Medical School, Boston, MA 02115; <sup>2</sup>Center for Regenerative Medicine (CIME) Udine Medical School, Udine 33100, Italy; <sup>3</sup>Department of Pathology, University of Trieste Medical School, Trieste 22500, Italy; <sup>4</sup>Cardiovascular Institute, Beth Israel Deaconess Medical Center, Harvard Medical School, Boston, MA 02115; <sup>5</sup>Center for Accelerator Mass Spectrometry, Lawrence Livermore National Laboratory, Livermore, CA 94551

Word count: 8476

Subject codes: [15] [131] [148] [154]

**Correspondence:** Piero Anversa, MD, Departments of Anesthesia and Medicine, and Cardiovascular Division, Brigham and Women's Hospital, Harvard Medical School, Boston, MA; panversa@partners.org

## **Abstract**

**Rationale:** The turnover of cardiomyocytes in the aging female and male heart is currently unknown, emphasizing the need to define human myocardial biology.

**Objective:** The effects of age and gender on the magnitude of myocyte regeneration and the origin of newly formed cardiomyocytes were determined.

**Methods and Results:** The interaction of myocyte replacement, cellular senescence, growth inhibition and apoptosis was measured in normal female (n=32) and male (n=42) human hearts collected from patients 19 to 104 years of age who died from causes other than cardiovascular diseases. A progressive loss of telomeric DNA in human cardiac stem cells (hCSCs) occurs with aging and the newly-formed cardiomyocytes inherit short telomeres and rapidly reach the senescent phenotype. Our data provide novel information on the superior ability of the female heart to sustain the multiple variables associated with the development of the senescent myopathy. At all ages, the female heart is equipped with a larger pool of functionally-competent hCSCs and younger myocytes than the male myocardium. The replicative potential is higher and telomeres are longer in female hCSCs than in male hCSCs. In the female heart, myocyte turnover occurs at a rate of 10%, 14% and 40% per year at 20, 60 and 100 years of age, respectively. Corresponding values in the male heart are 7%, 12% and 32% per year, documenting that cardiomyogenesis involves a large and progressively increasing number of parenchymal cells with aging. From 20 to 100 years of age, the myocyte compartment is replaced 15 times in women and 11 times in men.

**Conclusions:** The human heart is a highly dynamic organ regulated by a pool of resident hCSCs that modulate cardiac homeostasis and condition organ aging.

**Key Words:** Gender, Aging Myopathy, Humans, Myocyte Renewal

For 4 decades, the human heart has been considered a post-mitotic organ composed of a predetermined number of myocytes, which is established at birth and is preserved throughout life.<sup>1</sup> On this premise, the age of myocytes corresponds to the age of the organ and organism, i.e., cellular, organ and organism age coincide. Myocytes must age at the same rate and, at any given time, the heart is composed of a homogeneous population of cells of identical age. Because of this static view, aging has been construed as a time-dependent process that interacts with ischemic injury, hypertension, diabetes and other disorders, which together define the senescent cardiac phenotype.

Results from our laboratory and others have documented that a tissue specific stem cell resides in the human heart.<sup>2-5</sup> Human cardiac stem cells (hCSCs) are multipotent in vitro and in vivo and differentiate into cardiomyocytes, and vascular smooth muscle cells and endothelial cells organized in coronary vessels.<sup>6</sup> The recognition that hCSCs live in the heart and generate cardiac cell lineages has imposed a reevaluation of the current view of cardiac homeostasis, aging and pathology. A novel conceptual framework of the heart has emerged; the heart is a self-renewing organ characterized by resident hCSCs stored in niches. The niches control the physiological turnover of cardiac cells<sup>7</sup> mediated by migration and commitment of hCSCs that leave the niche structure to replace old, dying cells within the myocardium.<sup>3,6</sup>

The controversy on the growth reserve of the adult human heart has not been resolved and the extent of myocyte renewal claimed by different groups varies dramatically. A recent study, based on retrospective carbon 14 (<sup>14</sup>C) birth dating of cells, has claimed that ~1% and ~0.45% replacement of myocytes occurs annually in the human heart at 25 and 75 years of age, respectively.<sup>8</sup> These findings indicate that only 50% of myocytes are renewed during the entire life of the human heart, from birth to death, while an equal number lives as long as the organ and organism, up to 100 years of age and longer. Although the possibility of myocyte regeneration was confirmed, the actual magnitude of the process is in contrast with the level of myocyte apoptosis found in the adult human heart<sup>9</sup> and the progressive increase in myocyte loss that occurs with aging in humans.<sup>10</sup>

Therefore, we determined the interaction of myocyte regeneration, cellular senescence, growth inhibition and apoptosis in normal female and male human hearts, collected from patients, 19 to 104 years of age, who died from causes other than cardiovascular diseases. A large number of hearts was included to obtain a common denominator of the processes that regulate replication and death of ventricular myocytes. The average age of cardiomyocytes, their age distribution, turnover rate, and time to acquire the senescent phenotype were measured to define the biology of myocardial aging as a function of organ and organism lifespan.

## **Methods**

The percentage of senescent myocytes and the fraction of cells undergoing apoptosis were evaluated by the expression of p16<sup>INK4a</sup> and TdT labeling, respectively. The number of cycling and dividing myocytes was assessed by Ki67 and phospho-H3/aurora B kinase. An expanded Methods section is available in the online Data Supplement at <http://circres.ahajournals.org>.

## **Results**

### **Physiological Myocardial Aging**

In an attempt to avoid the effects of causes unrelated to the aging process, a series of variables were considered in the selection of the 74 human hearts studied. A stringent approach was followed to minimize the consequences on myocardial aging of unpredictable events that occur during the course of life together with the pathological manifestations of the heart and other organs.<sup>10</sup> These factors confound the etiology of the aging myopathy and its evolution. Therefore, specific selection criteria were introduced clinically, anatomically and histologically (Online Table I). The latter was particularly relevant, because multiple focal areas of myocardial damage and tissue fibrosis, indicative of extensive myocyte loss, are not detectable grossly and are frequently associated with an apparently normal cardiac weight, resulting from reactive hypertrophy of the remaining viable myocytes.

Cardiac aging was characterized by modest interstitial and perivascular fibrosis, occasional small foci of reparative fibrosis and lack of inflammatory infiltrates (Online Figure IA-IF). A certain degree of myocyte hypertrophy was present in the male myocardium while, in the female heart, cellular enlargement became apparent only in the advanced stages of life (Online Figure IG-IJ). In both genders, the aging heart had relatively intact coronary arteries or modest atherosclerosis with reductions in luminal diameter, known not to affect blood flow or coronary vascular resistance.<sup>11</sup>

### **Women and Men**

The predominant cause of death in our patient population was pulmonary infection, followed by rupture of cerebral and aortic aneurisms, traumatic injury, pulmonary thromboembolism, suicide and gastrointestinal hemorrhage (Online Table II). Other non-cardiovascular illnesses were also involved in a few cases. In the majority of patients, death occurred as a result of a disease state but pathology developed terminally and had, at most, little effect on the myocardium. When acute trauma was the fatal event, a complete medical history could not be obtained. However, the absence of a previous hospital record, and the lack of organ pathology at complete autopsy, which was confirmed by detailed histology, justified their inclusion in the study.

Thirty-two female and 42 male hearts were analyzed (Online Table II). From 19 to 49 years of age, 28 hearts were obtained and a similar number of cases (n=24) encompassed the age interval from 50 to 69 years. From 72 to 104 years, 22 cases were collected. Male hearts were more numerous at a younger age while, from 80 to 104 years, the number of female hearts (n=11) was nearly twice the number of male hearts (n=6). This difference may reflect the longer lifespan of women in the Western world.

Earlier quantitative studies of the aging human heart in women and men<sup>10</sup> have shown that from 17 to 89 years of age, nearly  $64 \times 10^6$  cardiomyocytes are lost per year in men while myocyte number does not change in the female heart up to 90 years of age. These observations have raised the question whether these remarkable differences in the aging-dependent adaptation of the myocardium according to gender reflect distinct degrees of myocyte turnover. A perfect balance appears to exist between myocyte renewal and death in women, while myocyte loss exceeds cell formation in men. Alternatively, myocyte turnover is extremely low in the female heart being essentially undetectable by morphometric protocols. Therefore, the critical determinants of cardiac homeostasis, i.e., ongoing myocyte death and regeneration, were measured in the aging heart of both sexes to define the characteristics of the myocardium at patient's death.

### **Myocyte Senescence and Death**

In the human heart, apoptosis is invariably coupled with the expression of the aging-associated protein p16<sup>INK4a</sup> that is a marker of replicative senescence and irreversible growth arrest of progenitor cells in various organs including the heart.<sup>12-14</sup> P16<sup>INK4a</sup>-positive myocyte nuclei were found at all ages in women and men (Online Figure IIA-IID); the specificity of the recorded signal was validated by spectral analysis (Online Figure IIE). The frequency of senescent myocytes was commonly higher in men than in women throughout life. In the oldest man, 104 years of age, 80% of myocytes expressed this nuclear protein. This was not the case in the oldest woman, 102 years of age, where a relevant proportion of myocytes, 45%, did not reach the senescent phenotype.

From 19 to 49, 50 to 69, and 72 to 104 years of age, the fraction of myocyte nuclei labeled by p16<sup>INK4a</sup> was 43%, 35% and 32% lower in women than in men, respectively (Figure 1A). From 19 to 104 years of age, the time-dependent increase in old myocytes was 0.68% per year in women and 0.89% per year in men; the 31% higher rate of accumulation of senescent myocytes in the aging male heart was significant (Figure 1B). In comparison with cellular senescence, myocyte apoptosis was relatively low but it occurred only in p16<sup>INK4a</sup>-positive cells (Online Figure IIF and IIG). Cell death was higher in men than in women at 19 to 49, 50 to 69 and 72 to 104 years of age (Figure 1C). However, the rate of increase in myocyte apoptosis with age did not differ with gender: 131 cells/10<sup>8</sup> per year in men and 123 cells/10<sup>8</sup> per year in women (Figure 1D).

Cell apoptosis is completed in all organs in less than 4 hours,<sup>15</sup> suggesting that these rates of cell death result in a massive loss of myocytes with aging. If we consider the number of cells present in the left ventricle in women and men at 20 years,<sup>10</sup> the myocardium would essentially disappear with time. In the absence of myocyte formation, only 5% of cardiomyocytes would persist at 63 and 48 years of age in women and men, respectively (Figure 1E). Thus, myocyte regeneration has to play a major role in the preservation of tissue mass and function of the aging human heart.

### **Aging and hCSCs**

The possibility that a certain degree of myocyte regeneration occurs in the human heart is currently accepted, but questions persist concerning the origin of newly formed cardiomyocytes. The mammalian heart contains a pool of c-kit-positive cells, which possess the fundamental properties of stem cells: they are self-renewing, clonogenic and multipotent in vitro and in vivo.<sup>3,6,7,12,16</sup> These findings point to resident stem cells as the source of myocyte renewal physiologically and pathologically. Studies in rodents have claimed that terminally-differentiated myocytes can be forced to reenter the cell cycle and divide.<sup>17-19</sup> However, this work fell short in documenting whether a mature myocyte, ~25,000  $\mu\text{m}^3$  in volume, increases its size during S phase and G2 phase, reaching ~50,000  $\mu\text{m}^3$  volume, and then divides giving rise to two daughter cells ~25,000  $\mu\text{m}^3$  each. Conversely, dividing myocytes are small poorly differentiated cells, resembling cycling amplifying myocytes in the process of acquiring the adult post-mitotic phenotype.<sup>20</sup> Genetic manipulations involving transgene constructs placed under the control of the  $\alpha$ -myosin heavy chain promoter<sup>17,18</sup> inevitably affect myocyte precursors and the pool of amplifying myocytes.<sup>21</sup>

Collectively, these observations support the notion that myocyte regeneration in the human heart is dictated by activation and commitment of resident hCSCs and a hierarchical organization of their progeny. According to this model of myocyte renewal, the acquisition of the myocyte phenotype involves sequentially the generation of myocyte progenitors and precursors, cycling amplifying myocytes and ultimately mature

post-mitotic parenchymal cells.<sup>3,6,7,16,20</sup> The quantitative assessment of this process requires the analysis of its various components (Online Figure IIIA-IIIC) and validation of the specificity of the recorded signals by spectral analysis (Online Figure IIID).

hCSCs are c-kit-positive primitive cells, negative for transcription factors, membrane and cytoplasmic proteins typical of cardiac cell lineages. Myocyte progenitors retain the stem cell antigen c-kit but express transcription factors specific of myocytes, GATA4, Nkx2.5 and MEF2C. Myocyte precursors are positive for c-kit, GATA4, Nkx2.5 and MEF2C and contain several contractile proteins. Amplifying myocytes are no longer positive for c-kit and sarcomeres progressively accumulate. This cell class proliferates and concurrently differentiates until the adult cell phenotype is reached and cell division is permanently suppressed.<sup>3,6,7,16,20</sup>

The number of hCSCs was similar in the young and middle-age female and male myocardium, but differed in the old heart (Figure 2A). In women, from 21 to 102 years of age, hCSCs increased at a rate of 2,300/10g per year, while, in men, from 19 to 104 years of age, hCSCs increased at a rate of 1,400/10g per year. This difference was statistically significant (Figure 2B). These values, however, do not consider the biological properties of hCSCs. Three variables dictate the number of functionally-competent hCSCs in the myocardium: **1.** Degree of cell replication; **2.** Length of the cell cycle; and **3.** Proportion of cells that have the ability to divide, or have acquired the senescent phenotype.

The cell cycle marker Ki67 was employed to measure the fraction of proliferating hCSCs, since this nuclear protein is coupled with karyokinesis and cytokinesis.<sup>3,12</sup> Comparable values were found in young hearts of both genders, while differences between women and men became apparent with age. Ki67-positive hCSCs increased 514/10<sup>6</sup> per year in women and 193/10<sup>6</sup> per year in men (Figure 2C and 2D; Online Figure IV); the 2.7-fold higher yearly rate of hCSC growth in women was significant.

The length of the cell cycle was determined in vitro in hCSCs obtained from the right atrial appendage of 4 patients, 2 men (age: 56 and 83 years) and 2 women (age: 50 and 72 years), who underwent coronary bypass surgery. hCSCs were pulse-labeled with BrdU for 20 min and cells were fixed at one hour intervals up to 48 hours to assess the percentage of labeled mitosis.<sup>22</sup> This parameter was derived from a total of 1,041 hCSCs in mitosis and plotted as a function of time. The duration of the cell cycle was comparable in the 4 determinations and averaged 26±4 hours (Figure 2E).

Senescent hCSCs were identified by the expression of p16<sup>INK4a</sup>.<sup>13</sup> This nuclear protein was detected more frequently in male than in female hCSCs at all ages (Figure 3A and 3B). However, the time-dependent increase in the rate of p16<sup>INK4a</sup>-positive hCSCs did not differ in the female and male heart (Figure 3C). Since the percentage of Ki67-positive cycling hCSCs and the duration of the cell cycle were similar in women and men, the number of hCSCs and the fraction of p16<sup>INK4a</sup>-negative cells were combined to yield the pool of functionally-competent hCSCs in the aging heart. Contrary to expectation, this variable increased in the old and senescent myocardium, although these changes were more dramatic in women than men (Figure 3D and 3E).

### **Ageing and hCSC Differentiation**

The compartment of myocyte progenitors and precursors increased as a function of age in both genders. Similar values were found in the young female and male heart while the

number of these cell classes together became progressively higher in women 50 years of age and older (Figure 4A). The rate of formation of myocyte progenitors and precursors was 11,000/10g per year in the female and 6,700/10g per year in the male myocardium (Figure 4B). Amplifying myocytes proliferate and accumulate structural proteins needed for their mechanical behavior and phenotypic maturation. Three markers were employed to characterize their growth behavior: Ki67, phospho-H3 and aurora B kinase. Ki67 is expressed in late G1, S, G2 and early mitosis and is not implicated in DNA repair.<sup>23</sup> Phospho-H3 is upregulated in late G2 and mitosis. It is highly phosphorylated at Ser10 during chromatin condensation and remains phosphorylated up to the end of telophase.<sup>24</sup> Aurora B kinase is associated with separating chromosomes throughout mitosis and it localizes at the cleavage furrow documenting cytokinesis.<sup>25</sup>

Amplifying myocyte nuclei labeled by Ki67, phospho-H3 and aurora B kinase were found in young, middle-age and senescent hearts (Figure 4C-4F), and aging was characterized by a time-dependent increase in the generation of this cell class in both genders. Levels of Ki67 (Figure 4G) and phospho-H3 (Figure 4H) were comparable in young females and males, but differed later in life. The pool of amplifying myocytes and the fraction of mitotic myocytes were, respectively, 1.7-fold and 1.5-fold higher in old women than men (Figure 4G and 4H), pointing to enhanced myocyte renewal in the female LV. Importantly, the rate of increase in amplifying and mitotic myocytes per year was higher in the female than male myocardium (Figure 4I and 4J). In agreement with previous results,<sup>26</sup> the proportion of mononucleated and binucleated myocytes did not change from 19 to 104 years of age (Online Figure V). Thus, Ki67, phospho-H3 and aurora B kinase labeling were all markers of cell replication, indicating that cardiac aging was characterized by a significant degree of myocyte regeneration.

### **Aging and Post-Mitotic Myocytes**

Young, non-dividing myocytes were identified by the lack of expression of Ki67 and p16<sup>INK4a</sup>. This myocyte class was consistently higher in women than men 50 years of age and older (Figure 5A). In both genders, an inverse relationship was found between young myocytes and aging. The rate of decrease of young myocytes was 0.69% per year in women and 0.89% per year in men and this difference was significant (Figure 5B). When the rate of decrease in the fraction of young myocytes (Figure 5B) was compared with the rate of generation of senescent cells (see Figure 1B), it became evident that activation and differentiation of hCSCs was insufficient to maintain the youth of the organ and, possibly, the structural integrity of the aging myocardium. The time-dependent decrease in young post-mitotic myocytes was coupled with an age-dependent increase in senescent hCSCs (Online Figure VI). However, this negative effect was more apparent in the male heart, which also lost a large number of parenchymal cells.<sup>10</sup> Conversely, the myocyte compartment is preserved in the old female heart.<sup>10</sup>

### **Nuclear Ploidy and Cell Fusion**

To strengthen the notion that dividing myocytes were actually the progeny of hCSCs, the presence of ploidy and cell fusion was determined by measuring, respectively, DNA content by confocal microscopy and the number of sex chromosomes by Q-FISH.<sup>3,12,14</sup> These determinations were restricted to 10 young, 5 females and 5 males, and 10 old, 5 females and 5 males, hearts.

In the majority of cases,  $2n$  diploid DNA content was found in all samples (Figure 6A). The fraction of myocyte nuclei with DNA content higher than  $2n$  and lower than  $4n$

reflected replicating cells expressing Ki67. Tetraploid and octaploid myocyte nuclei increased with age in both the female and male heart (Figure 6B). These polyploid cells were negative for Ki67 excluding that they represented cycling cells in G2. Additionally, myocyte nuclei contained almost exclusively two X-chromosomes or one X and one Y chromosome, ruling out cell fusion (Figure 6C). Myocyte nuclei that contained two sets of sex chromosomes represented dividing cells positive for phospho-H3 (Figure 6D). Thus, forming myocytes were predominantly the descendants of hCSCs.

### **Hierarchical Organization of the Myocyte Progeny**

Two independent mathematical models were introduced to determine the age and turnover of cardiomyocytes: the hierarchical and population dynamics models.<sup>27,28</sup> The hierarchical model allows the characterization of the biological processes occurring at the level of the controlling cells, i.e., the hCSCs, and their destiny following activation and differentiation.<sup>27</sup> By this approach, the number of cardiomyocytes generated by hCSCs in a specific timeframe can be derived, together with their average age.

In both women and men, the magnitude of entry of hCSCs into the cell cycle was similar in the young and middle-age heart: ~2,900 cells/10g of myocardium per day in the young heart and ~6,500 cells/10g of myocardium per day in the middle-age heart. In the old heart, this value was significantly higher in women, 17,000 cells/10g of myocardium per day, than in men, 9,400 cells/10g of myocardium per day (Figure 7A). There were no differences in the number of mature myocytes generated by one female or one male hCSCs at each of the three age intervals examined (Figure 7B). However, in young, middle-age and old women and men, activation and differentiation of a single hCSC led in 5.6 (young), 5.8 (middle-age) and 6.5 (old) days to the generation of 36, 41 and 66 mature myocytes, respectively. These values are dependent on the length of the cell cycle (see Figure 2E) and the number of divisions required by hCSCs to go through, before mature myocytes are formed (Figure 7C). If the same young, middle-age and old hCSCs experienced constant activation, 190, 215 and 305 mature myocytes were formed in one month, and 2,300, 2,600 and 3,600 in one year, respectively (Figure 7D). These data, in combination with the number of functionally-competent hCSCs in the heart (see Figure 3B), allowed us to determine the age-dependent changes in the rate of cardiomyocyte generation in women and men. During the course of life, the rate of myocyte formation increased by 2,500,000/10g per year in females and 1,000,000/10g per year in males (Figure 7E).

In the young, middle age and old heart, myocyte volume was, respectively, 22,000, 23,000 and 23,000  $\mu\text{m}^3$  in women, and 23,000, 26,000 and 29,000  $\mu\text{m}^3$  in men.<sup>10</sup> The number of cardiomyocytes per 10g of myocardium was then obtained to compute the fraction of myocytes replaced per year. Annually, myocyte turnover involved 8%, 14% and 31% of cells in young, middle-age and old women, and 7%, 13% and 18% of cells in young, middle-age and old men, respectively (Online Figure VII). The average age of myocytes was 7 years in young, 3 years in middle-age and 2 years in the old female heart. Corresponding values in men were 8, 4 and 3 years (Online Figure VIII).

### **Population Dynamics and Distribution of Myocyte Age**

The model of population dynamics, which is based on the differential equation of age density function,<sup>28</sup> does not utilize the information related to the behavior and fate of hCSCs. It is based on the knowledge of the various classes of cardiomyocytes to define their different age. This parameter permits also the computation of myocyte turnover and the measurement of the average myocyte age at any point in time during the course of

life. Thus, the hierarchical and population dynamics models provide complementary information and are expected to generate comparable data. The results on cycling and mitotic myocytes, together with the values of myocyte death, allowed us to compute the average birth date and distribution of ages of parenchymal cells in the female and male heart. Organ age inversely correlated with myocyte age in both genders; young hearts had older myocytes than senescent hearts. Moreover, the middle-age and old female heart was composed of younger cells than the male heart. The average age of myocytes in young, middle-age and old women was 7, 3.5 and 2.5 years, respectively. Values in men were 8, 5 and 3 years (Online Figure IX). The rate of myocyte renewal was 6%, 15% and 37% per year in young, middle age and old women, and 5%, 13% and 20% per year in young, middle age and old men, respectively (Online Figure X).

These findings mimicked the results obtained independently with the model of hierarchically structured cell populations (see Online Figures VII and VIII), so that the data generated by these two approaches were combined to yield the extent of myocyte replacement in the heart. Cell renewal accounted, respectively, for 7%, 15% and 34% of myocytes in young, middle-age and old women, and 6%, 13% and 19% of myocytes in young, middle-age and old men (Figure 7F).

None of the myocytes present in the female and male heart at 20 years had the same age of the organ. The majority of cells, 72%, were 3-12 years old; a small fraction, 13%, was younger than 3 years and a similar proportion, 15%, was older than 12 years. With the exception of a 23 years old male heart in which 1.2% of myocytes were 23 years old, all parenchymal cells in the remaining 73 cases were younger than the organ and organism (Online Figure IX).

A gender shift in the age distribution of myocytes became apparent at 50 years of age and increased with time (Figure 8A). In the oldest woman, 102 years old, and man, 104 years old, different proportions of young and old cells were found. Myocyte age in female and male heart varied from 0 to 9 years, and 0 to 12 years, respectively (Figure 8B). Cells younger than 2 years comprised 37% and 29% of the myocyte population in women and men, respectively. Conversely, myocytes older than 5 years constituted 6% of the female and 20% of the male myocardium (Figure 8B).

### **Telomere Length in hCSCs and Myocytes**

There was an apparent paradox between the increase in the number of senescent myocytes and the increase in myocyte renewal with aging. The older the organ the younger was the age of the myocyte compartment. In an attempt to clarify this conundrum, telomere length was measured by Q-FISH in c-kit-positive hCSCs and myocytes of 20 hearts, 5 each from young and old women and men (Figure 9A-9C). The objective was to determine whether aged hCSCs generated an old myocyte progeny.

The length of telomeres in hCSCs and myocytes showed in each case a consistent pattern. If hCSCs exhibited long telomeres, myocytes revealed comparable telomere length. Similarly, hCSCs with short telomeres were paralleled by myocytes with severe telomere attrition (Figure 9D). Telomeric shortening occurred with aging in hCSCs of both genders, although these changes were more dramatic in men than in women. Myocytes behaved in an identical manner (Figure 9D). Importantly, in all 10 old hearts, there was a small fraction of hCSCs and myocytes with telomeres of normal length, 8-12kbp (Online Figure XI). Possibly, older hCSCs generated an older myocyte progeny, which rapidly acquired the senescent phenotype. This notion was supported by the

documentation in the old hearts of myocyte precursors with telomeres less than 4kbp (Figure 10A-10C). These cell classes established a lineage relationship between aged hCSCs and aged myocytes.

These observations suggested that the time required by newly formed myocytes to become senescent varied with age. The number of years needed by a cardiomyocyte to express p16<sup>INK4a</sup> was determined by combining the average age of cardiomyocytes with the percentage of cells positive for the senescence-associated protein. This time interval decreased progressively in aging women and men, although it was more rapid in male than in female myocytes. In a 20 years old heart, nearly 14 years were necessary for myocytes to become p16<sup>INK4a</sup>-positive, while in a 90 years old heart, myocytes reached the old phenotype in approximately 2 years (Figure 10D).

## Discussion

The recognition that the human heart harbors resident multipotent hCSCs capable of forming cardiomyocytes and coronary vessels<sup>2-5</sup> has posed the demanding question concerning the role of these cells in myocardial aging.<sup>29</sup> Results in the present study provide compelling evidence in favor of the notion that the aging myopathy is a stem cell disease. A progressive loss of telomeric DNA in hCSCs occurs with aging and, although the pool of functionally-competent hCSCs expands with time and generates a larger myocyte progeny, the newly-formed cardiomyocytes inherit short telomeres and rapidly reach the senescent cell phenotype. The expression of p16<sup>INK4a</sup> becomes apparent and apoptosis is markedly increased. Deficient hCSCs generate old cardiomyocytes which, as shown in animal models, have severely depressed mechanical performance and alterations in calcium metabolism.<sup>30,31</sup>

Collectively, our data challenge current views on the mechanisms involved in the development of the aging myopathy in women and men. A decrease in myocyte turnover in the old heart has been claimed,<sup>8</sup> but our findings indicate that myocyte regeneration increases as a function of age, and the age of cardiomyocytes does not coincide with the age of the organ and organism. This discrepancy becomes more apparent in the senescent myocardium in which a large proportion of myocytes is approximately 5 years old or younger in both women and men. The older the human heart the younger is its myocyte compartment. From 19 to 104 years of age, essentially none of the myocytes present at birth are preserved in the young adult, middle age, and senescent heart. These findings question the contention that 50% of cardiomyocytes are not replaced during the entire lifespan in humans,<sup>8</sup> suggesting that a large proportion of cells survives and retains its function for more than 100 years. This rather static view of the heart is disputed here by offering a highly dynamic perspective of myocardial biology and aging.

## hCSCs and the Aging Heart

Results in the present study indicate that hCSC aging conditions myocardial aging; chronological age leads to telomeric attrition in hCSCs, which generate a progeny that rapidly attains the senescent phenotype. Daughter cells acquire the shortened telomeres of maternal hCSCs and, after a few rounds of division and terminal differentiation, express p16<sup>INK4a</sup> in nearly 2 years. The pool of old cardiomyocytes progressively increases defining the aging myopathy. Telomere length reflects the past replicative history and cumulative oxidative DNA damage occurring during the life cycle of the cell.<sup>32</sup> hCSC function is regulated by telomerase activity and telomere length.<sup>3</sup> Telomerase activity delays but cannot prevent telomere erosion, which is mediated by downregulation of telomerase, reactive oxygen species and loss of telomere-related

proteins.<sup>12,33</sup> Shortening of telomeres beyond a critical length triggers cellular senescence, which corresponds to irreversible growth arrest in G1 with loss of specialized functions, including cell proliferation, migration and differentiation. Suggestive evidence in humans and genetically manipulated mice<sup>34-36</sup> points to shortening of telomeres, as a critical determinant of cellular senescence and, possibly, organ aging. Importantly, a lineage relationship was found between hCSCs with short telomeres and the formation of old myocytes.

Of great interest, a pool of hCSCs with intact telomeres, 8-12 kbp, was found in the female and male heart at 90 to 104 years of age. This category of hCSCs with high growth reserve is expected to generate a young myocyte progeny within the senescent heart. Since each division of hCSCs results in the loss of ~130bp of telomeric DNA,<sup>3</sup> an extremely large number of cardiomyocytes can be formed by these cells, before critical telomeric shortening and growth arrest occur.<sup>37</sup> The heterogeneity in telomere length among hCSCs raises challenging questions. The possibility can be advanced that hCSCs with long telomeres are better equipped to sustain oxidative stress or are nested in well-protected areas of the myocardium. However, the variability in telomere length of hCSCs may be dictated by their different cycling history. In a manner similar to other tissue specific stem cells,<sup>37,38</sup> the compartment of hCSCs may be composed of a subset of quiescent cells with preserved telomere integrity and a pool of highly proliferating cells that maintain organ homeostasis but lose telomeric DNA at each round of division.

Alternatively, in the old heart, hCSCs with long telomeres may reflect a residual compartment of mother cells which retained the immortal DNA during division. If this hypothesis of stem cell growth is valid,<sup>39,40</sup> stem cell division would be characterized by asymmetric segregation of chromatids so that one daughter cell contains only the old intact DNA templates, and the other daughter cell contains chromatids composed exclusively of the newly synthesized DNA strands. The process of non-random segregation of chromatids would attenuate the accumulation of spontaneous mutations and telomere attrition.<sup>39</sup> Whether these hCSCs can be selectively activated to repopulate the senescent heart with young, mechanically efficient cardiomyocytes remains an important unanswered question.

### **Gender and Myocardial Aging**

Data in this study provide novel information on the superior ability of the female heart to sustain the multiple variables associated with the aging process and the development of the senescent myopathy. At all ages, the female heart is equipped with a larger pool of functionally-competent hCSCs and younger myocytes than the male myocardium. The replicative potential is higher and telomeres are longer in female hCSCs than in male hCSCs. Animal studies have shown that the IGF-1-IGF-1 receptor system is present in CSCs at very old age,<sup>31</sup> and overexpression of IGF-1 in cardiomyocytes prevents the manifestations of the senescent cardiac phenotype and heart failure.<sup>41</sup> Additionally, the IGF-1-IGF-1 receptor axis is enhanced in female myocytes<sup>42</sup> and it may condition the favorable outcome of age in this gender.

Estrogens phosphorylate IGF-1 receptors<sup>43</sup> mimicking the effects of IGF-1, a powerful inducer of CSC division and survival.<sup>31,41</sup> In postmenopausal women and throughout life in men, estrogen is synthesized in extragonadal organs including bone, cartilage, adipose tissue, skin, breast and heart.<sup>44</sup> With aging, estrogen loses its circulating generalized function and works mainly at the local level as a paracrine, autocrine or intracrine factor. Estrogen induces transcription of the catalytic subunit of the telomerase

protein (TERT), since an estrogen response element is present in the TERT promoter.<sup>45</sup> Additional downstream effector pathways of estrogen involve the activation of PI3 kinase/Akt cascade, which exerts multiple beneficial effects on cardiac performance and biology.<sup>46</sup>

### **Aging and Myocyte Turnover**

The results of the current study indicate that myocyte regeneration in the physiologically aging heart takes place at previously unexpected levels in both women and men. In view of their similarity, the data obtained by the hierarchical model of myocyte renewal and those based on population dynamics were combined. In the female heart, myocyte replacement occurs at a rate of 10%, 14% and 40% per year at 20, 60 and 100 years of age, respectively. Corresponding values in the male heart are 7%, 12% and 32% per year, documenting that myocyte turnover involves a large and progressively increasing number of parenchymal cells with aging.

In the last two decades, several lines of evidence have been obtained in favor of the regeneration potential of the young, adult and aged myocardium.<sup>3,10,12,14,47,48</sup> Data on retrospective <sup>14</sup>C birth dating of myocytes have strengthened the notion that myocyte formation occurs in humans, but at a significantly lower rate than that reported here.<sup>8</sup> Hopefully, this work will resolve the long debate which has divided the scientific community in strong opponents and passionate supporters of the regenerative potential of the human heart, offering a more biologically valid understanding of cardiac homeostasis and repair. A common ground can now be found to translate this different perspective of cardiac biology into the development of novel strategies for the management of the human disease. However, the magnitude of the process, the effects of age on the extent of myocyte renewal and the origin of newly formed cardiomyocytes is a matter of controversy.

These crucial issues have been answered in the current study in which a series of integrated analyses have been performed. They included measurements of the number of hCSCs, the fraction of cycling hCSCs and the length of their cell cycle to evaluate the rate of entry of hCSCs into the growth phase. Additionally, the number of forming myocytes at increasing levels of lineage specification was assessed. They involved myocyte progenitors, myocyte precursors and amplifying myocytes to establish the number of divisions that one hCSC undergoes before the adult post-mitotic cell phenotype is acquired. These parameters were introduced into the equation reflecting the growth kinetics of hierarchically structured cell populations, yielding a high degree of myocyte turnover, which increased further with age. From 20 to 100 years of age, the myocyte compartment was replaced completely 15 times in women and 11 times in men.

### **Myocyte Birth Dating**

The striking differences between our results and the data derived from the integration of <sup>14</sup>C in the DNA of myocyte nuclei impose a careful evaluation of this published report.<sup>8</sup> Retrospective birth dating of human myocardium DNA by <sup>14</sup>C mirrors the incorporation of thymidine analogs in animal models, an analysis which has only been rarely possible in human beings and, thus far, has been restricted to the brain<sup>49</sup> and more recently to the heart.<sup>14</sup> An inherent limitation of <sup>14</sup>C birth dating is related to the need to introduce mathematical models with assumptions that affect the computed cell turnover values.<sup>8</sup> The scenario chosen presumed that the number of myocytes in the heart was constant and that cells turned over at a near constant rate. This form of invariant growth defines parenchyma in a steady state in which cell death is compensated by cell regeneration in

young healthy individuals. However, this steady state scenario poorly represents the biology of aging in men where nearly  $64 \times 10^6$  cardiomyocytes are lost per year. Furthermore, since women do not lose cardiomyocytes as they age like men,<sup>10</sup> different models should be used to reflect the changing cell populations. Importantly, myocyte number increases postnatally,<sup>14,50</sup> and cell loss typically occurs with cardiac diseases.<sup>9</sup>

These limitations were avoided in the current study by evaluating a large number of non-pathologic aging hearts of both sexes. In contrast to the single determination of  $^{14}\text{C}$  made in the earlier report,<sup>8</sup> multiple variables were measured and two distinct mathematical models were employed. In both cases, the data concurred and were consistent with previous results.<sup>14,20</sup> Another problem with the previous work involves the use of troponin I expression as a marker for the isolation of a representative pool of myocyte nuclei. However, the presence of troponin I identifies almost exclusively a population of p16<sup>INK4a</sup>-positive senescent cells which exhibit marked alterations in the permeability of nuclear pore complexes.<sup>14</sup> Additionally, the percentage of p16<sup>INK4a</sup>-positive myocytes varies dramatically with age and cardiac diseases.<sup>12,48</sup> The failure to directly measure the  $^{14}\text{C}$  content of non-myocytes and the unrealistically high myocyte fraction varying from 29% to 60% of the cardiac cell pool, although accounting for ~20% of the cells,<sup>1</sup> obscure the non-specificity of the nuclear marker used to sort myocytes. Data from a small number of samples were used to generate a model despite non-physical implications of the non-myocyte population. In contrast, we utilized multiple markers of cell turnover in a large number of healthy hearts spanning a large age range to measure and model much higher cell turnover.

### **Acknowledgment**

This work was supported by NIH grants. Silvana Bardelli was supported by a grant from Cardiocentro Ticino, Lugano, Switzerland. Work was performed in part under the auspices of the U.S. Department of Energy by Lawrence Livermore National Laboratory under Contract DE-AC52-07NA27344.

### **Disclosures**

None

### **References**

1. Rubart M, Field LJ. Cardiac regeneration: repopulating the heart. *Annu Rev Physiol.* 2006;68:29-49.
2. Smith RR, Barile L, Cho HC, Leppo MK, Hare JM, Messina E, Giacomello A, Abraham MR, Marbán E. Regenerative potential of cardiosphere-derived cells expanded from percutaneous endomyocardial biopsy specimens. *Circulation.* 2007;115:896-908.
3. Bearzi C, Rota M, Hosoda T, Tillmanns J, Nascimbene A, De Angelis A, Yasuzawa-Amano S, Trofimova I, Siggins RW, Lecapitaine N, Cascapera S, Beltrami AP, D'Alessandro DA, Zias E, Quaini F, Urbanek K, Michler RE, Bolli R, Kajstura J, Leri A, Anversa P. Human cardiac stem cells. *Proc Natl Acad Sci USA.* 2007;104:14068-14073.
4. Kubo H, Jaleel N, Kumarapeli A, Berretta RM, Bratinov G, Shan X, Wang H, Houser SR, Margulies KB. Increased cardiac myocyte progenitors in failing human hearts. *Circulation.* 2008;118:649-657.
5. Itzhaki-Alfia A, Leor J, Raanani E, Sternik L, Spiegelstein D, Netser S, Holbova R, Pevsner-Fischer M, Lavee J, Barbash IM. Patient characteristics and cell

- source determine the number of isolated human cardiac progenitor cells. *Circulation*. 2009;120:2559-2566.
6. Hosoda T, D'Amaro D, Cabral-Da-Silva MC, Zheng H, Padin-Iruegas ME, Ogorek B, Ferreira-Martins J, Yasuzawa-Amano S, Amano K, Ide-Iwata N, Cheng W, Rota M, Urbanek K, Kajstura J, Anversa P, Leri A. Clonality of mouse and human cardiomyogenesis in vivo. *Proc Natl Acad Sci USA*. 2009;106:17169-17174.
  7. Urbanek K, Cesselli D, Rota M, Nascimbene A, De Angelis A, Hosoda T, Bearzi C, Boni A, Bolli R, Kajstura J, Anversa P, Leri A. Stem cell niches in the adult mouse heart. *Proc Natl Acad Sci USA*. 2006;103:9226-9231.
  8. Bergmann O, Bhardwaj RD, Bernard S, Zdunek S, Barnabé-Heider F, Walsh S, Zupicich J, Alkass K, Buchholz BA, Druid H, Jovinge S, Frisén J. Evidence for cardiomyocyte renewal in humans. *Science*. 2009;324:98-102.
  9. Olivetti G, Abbi R, Quaini F, Kajstura J, Cheng W, Nitahara JA, Quaini E, Di Loreto C, Beltrami CA, Krajewski S, Reed JC, Anversa P. Apoptosis in the failing human heart. *N Engl J Med*. 1997;336:1131-1141.
  10. Olivetti G, Giordano G, Corradi D, Melissari M, Lagrasta C, Gambert SR, Anversa P. Gender differences and aging: effects on the human heart. *J Am Coll Cardiol*. 1995;26:1068-1079.
  11. Bache RJ, Dymek DJ. Local and regional regulation of coronary vascular tone. *Prog Cardiovasc Dis* 1981;24:191-212.
  12. Urbanek K, Torella D, Sheikh F, De Angelis A, Nurzynska D, Silvestri F, Beltrami CA, Bussani R, Beltrami AP, Quaini F, Bolli R, Leri A, Kajstura J, Anversa P. Myocardial regeneration by activation of multipotent cardiac stem cells in ischemic heart failure. *Proc Natl Acad Sci USA*. 2005;102:8692-8697.
  13. Beausejour CM, Campisi J. Ageing: balancing regeneration and cancer. *Nature*. 2006;443:404-405.
  14. Kajstura J, Urbanek K, Perl S, Hosoda T, Zheng H, Ogórek B, Ferreira-Martins J, Goichberg P, Rondon-Clavo C, Sanada F, D'Amaro D, Rota M, Del Monte F, Orlic D, Tisdale J, Leri A, Anversa P. Cardiomyogenesis in the adult human heart. *Circ Res*. 2010;107:305-315.
  15. De Saint-Hubert M, Prinsen K, Mortelmans L, Verbruggen A, Mottaghy FM. Molecular imaging of cell death. *Methods*. 2009;48:178-187.
  16. Beltrami AP, Barlucchi L, Torella D, Baker M, Limana F, Chimenti S, Kasahara H, Rota M, Musso E, Urbanek K, Leri A, Kajstura J, Nadal-Ginard B, Anversa P. Adult cardiac stem cells are multipotent and support myocardial regeneration. *Cell*. 2003;114:763-776.
  17. Pasumarthi KB, Nakajima H, Nakajima HO, Soonpaa MH, Field LJ. Targeted expression of cyclin D2 results in cardiomyocyte DNA synthesis and infarct regression in transgenic mice. *Circ Res*. 2005;96:110-118.
  18. Kühn B, del Monte F, Hajjar RJ, Chang YS, Lebeche D, Arab S, Keating MT. Periostin induces proliferation of differentiated cardiomyocytes and promotes cardiac repair. *Nat Med*. 2007;13:962-969.
  19. Bersell K, Arab S, Haring B, Kühn B. Neuregulin1/ErbB4 signaling induces cardiomyocyte proliferation and repair of heart injury. *Cell*. 2009;138:257-270.
  20. Anversa P, Kajstura J, Leri A, Bolli R. Life and death of cardiac stem cells: a paradigm shift in cardiac biology. *Circulation*. 2006;113:1451-1463.
  21. Bailey B, Izarra A, Alvarez R, Fischer KM, Cottage CT, Tuck S, Quijada P, Gude N, Alvarez R, Muraski J, Sussman MA. Cardiac stem cell genetic engineering using the alpha-MHC promoter. *Regen Med*. 2009;4:823-833.

22. Baserga R. The cell cycle. In: Baserga R, ed. *The Biology of Cell Reproduction*. Cambridge, Mass: Harvard University Press; 1985:3-21.
23. Scholzen T, Gerdes J. The Ki-67 protein: from the known and the unknown. *J Cell Physiol*. 2000;182:311-322.
24. Hendzel MJ, Wei Y, Mancini MA, Van Hooser A, Ranalli T, Brinkley BR, Bazett-Jones DP, Allis CD. Mitosis-specific phosphorylation of histone H3 initiates primarily within pericentromeric heterochromatin during G2 and spreads in an ordered fashion coincident with mitotic chromosome condensation. *Chromosoma* 1997;106:348-360.
25. Birkenfeld J, Nalbant P, Bohl BP, Pertz O, Hahn KM, Bokoch GM. GEF-H1 modulates localized RhoA activation during cytokinesis under the control of mitotic kinases. *Dev Cell*. 2007;12:699-712.
26. Olivetti G, Cigola E, Maestri R, Corradi D, Lagrasta C, Gambert SR, Anversa P. Aging, cardiac hypertrophy and ischemic cardiomyopathy do not affect the proportion of mononucleated and multinucleated myocytes in the human heart. *J Mol Cell Cardiol*. 1996;28:1463-1477.
27. Savill NJ. Mathematical models of hierarchically structured cell populations under equilibrium with application to the epidermis. *Cell Prolif*. 2003;36:1-26.
28. Milner FA, Rabbio G. Rapidly converging numerical algorithms for models of population dynamics. *J Math Biol*. 30: 733-753.
29. Lakatta EG. Age-associated cardiovascular changes in health: impact on cardiovascular disease in older persons. *Heart Fail Rev*. 2002;7:29-49.
30. Capasso JM, Fitzpatrick D, Anversa P. Cellular mechanisms of ventricular failure: myocyte kinetics and geometry with age. *Am J Physiol*. 1992;262:H1770-H1781.
31. Gonzalez A, Rota M, Nurzynska D, Misao Y, Tillmanns J, et al. (2008) Activation of cardiac progenitor cells reverses the failing heart senescent phenotype and prolongs lifespan. *Circ Res* 102: 597-606.
32. Blasco MA. Telomere length, stem cells and aging. *Nat Chem Biol*. 2007;3:640-649.
33. Collado M, Blasco MA, Serrano M. Cellular senescence in cancer and aging. *Cell*. 2007;130:223-233.
34. Leri A, Franco S, Zacheo A, Barlucchi L, Chimenti S, et al. (2003) Ablation of telomerase and telomere loss leads to cardiac dilatation and heart failure associated with p53 upregulation. *EMBO J*. 22: 131-139.
35. Blasco MA. Mice with bad ends: mouse models for the study of telomeres and telomerase in cancer and aging. *EMBO J*. 2005;24:1095-1103.
36. Armanios M. Syndromes of telomere shortening. *Annu Rev Genomics Hum Genet*. 2009;10:45-61.
37. Van Ziffle JA, Baerlocher GM, Lansdorp PM. Telomere length in subpopulations of human hematopoietic cells. *Stem Cells*. 2003;21:654-660.
38. Blanpain C, Fuchs E. Epidermal homeostasis: a balancing act of stem cells in the skin. *Nat Rev Mol Cell Biol*. 2009;10:207-217.
39. Rando TA. The immortal strand hypothesis: segregation and reconstruction. *Cell*. 2007;129:1239-1243.
40. Lansdorp PM. Immortal strands? Give me a break. *Cell*. 2007;129:1244-1247.
41. Torella D, Rota M, Nurzynska D, Musso E, Monsen A, Shiraishi I, Zias E, Walsh K, Rosenzweig A, Sussman MA, Urbanek K, Nadal-Ginard B, Kajstura J, Anversa P, Leri A. Cardiac stem cell and myocyte aging, heart failure, and insulin-like growth factor-1 overexpression. *Circ Res*. 2007;94:514-524.

42. Leri A, Kajstura J, Li B, Sonnenblick EH, Beltrami CA, et al. (2000) Cardiomyocyte aging is gender-dependent: the local IGF-1-IGF-1R system. *Heart Dis.* 2: 108-115.
43. Richards RG, DiAugustine RP, Petrusz P, Clark GC, Sebastian J. Estradiol stimulates tyrosine phosphorylation of the insulin-like growth factor-1 receptor and insulin receptor substrate-1 in the uterus. *Proc Natl Acad Sci USA.* 1996;93:12002-12007.
44. Simpson ER. Sources of estrogen and their importance. *J Steroid Biochem Mol Biol.* 2003;86:225-230.
45. Kyo S, Takakura M, Kanaya T, Zhuo W, Fujimoto K, Nishio Y, Orimo A, Inoue M. Estrogen activates telomerase. *Cancer Res.* 1999;59:5917-5921.
46. Rota M, Boni A, Urbanek K, Padin-Iruegas ME, Kajstura TJ, Fiore G, Kubo H, Sonnenblick EH, Musso E, Houser SR, Leri A, Sussman MA, Anversa P. Nuclear targeting of Akt enhances ventricular function and myocyte contractility. *Circ Res.* 2005;97:1332-1341.
47. Beltrami AP, Urbanek K, Kajstura J, Yan SM, Finato N, Bussani R, Nadal-Ginard B, Silvestri F, Leri A, Beltrami CA, Anversa P. Evidence that human cardiac myocytes divide after myocardial infarction. *N Engl J Med.* 2001;344:1750-1757.
48. Urbanek K, Quaini F, Tasca G, Torella D, Castaldo C, Nadal-Ginard B, Leri A, Kajstura J, Quaini E, Anversa P. Intense myocyte formation from cardiac stem cells in human cardiac hypertrophy. *Proc Natl Acad Sci USA.* 2003;100:10440-10445.
49. Eriksson PS, Perfilieva E, Björk-Eriksson T, Alborn AM, Nordborg C, Peterson DA, Gage FH. Neurogenesis in the adult human hippocampus. *Nat Med.* 1998;4:1313-1317.
50. Rakusan K. Cardiac growth, maturation, and aging. In: Zak R, ed. *Growth of the Heart in Health and Disease.* New York, NY: Raven Press; 1984:131-164.

## Legends to Figures

**Figure 1. Aging and myocyte senescence and death.** **A**, The fraction of p16<sup>INK4a</sup>-positive myocytes is consistently lower in women than men. **B**, The rate of increase in the fraction of p16<sup>INK4a</sup>-positive myocytes with age is lower in the female than in the male LV. **C**, The fraction of apoptotic myocytes in the LV is lower in women than men. F: female; M: male. \*p<0.05 vs. F. **D**, The rate of increase of apoptotic myocytes with age is similar in the female and male LV. **E**, At 20 years of age, the female (red) and male (blue) LV contains 4 and 6 x 10<sup>9</sup> cardiomyocytes, respectively. Curves are derived by combining the yearly levels of apoptosis shown in panel D and the prediction that cell death lasts 4 hours (see ref. 15). In the absence of cell regeneration, 5% of LV myocytes (200 x 10<sup>6</sup> in the female LV and 300 x 10<sup>6</sup> in the male LV) would be left at 63 and 48 years of age in the female and male LV, respectively.

**Figure 2. Aging and hCSC growth.** **A**, The number of lineage negative (Lin<sup>neg</sup>) c-kit-positive (c-kit<sup>pos</sup>) hCSCs/10g of myocardium increases with age more in women than men. F: female; M: male. \*p<0.05 vs. F. **B**, The rate of increase of Lin<sup>neg</sup>-c-kit<sup>pos</sup> hCSCs with age is higher in the female than in the male LV. **C**, The fraction of cycling Lin<sup>neg</sup>-c-kit<sup>pos</sup> hCSCs in the LV is higher in middle-age and old women than men. F: female; M: male. \*p<0.05 vs. F. **D**, The rate of increase of cycling Lin<sup>neg</sup>-c-kit<sup>pos</sup> hCSCs with age is higher in the female than in the male LV. **E**, BrdU labeled (white) c-kit-positive (green)

hCSCs at different stages of mitosis. The fraction of BrdU-labeled mitoses was plotted as a function of time (h: hours). Individual values are shown together with mean±SD.

**Figure 3. Aging and hCSC senescence.** **A**, Example of p16<sup>INK4a</sup>-positive hCSC (white, arrow). **B**, The fraction of p16<sup>INK4a</sup>-positive hCSCs is consistently lower in women than men. F: female; M: male. \*p<0.05 vs. F. **C**, The rate of increase in the fraction of p16<sup>INK4a</sup>-positive hCSCs with age is similar in the female and male LV. **D**, The number of functionally-competent hCSCs/10g of LV is higher in women than men at all ages. **E**, The rate of increase in the number of functionally-competent hCSCs/10g of LV with age is higher in women than men. Age and gender are indicated in panel A.

**Figure 4. Aging, myocyte progenitors and precursors, and amplifying myocytes.** **A**, The number of myocyte progenitors-precursors/10g of myocardium increases with age more in women than men. F: female; M: male. \*p<0.05 vs. F. **B**, The rate of increase of myocyte progenitors-precursors with age is higher in the female than in the male LV. **C-F**, Small amplifying myocytes are positive for phospho-H3 (C and D: white, arrows) and aurora B kinase (E and F: white, arrows). In panel F, aurora B kinase is located in the two sets of telophase chromosomes and at the cleavage furrow of the dividing myocyte (arrowhead). Insets in C-F illustrate the organization of chromosomes in the dividing cells. **G** and **H**, The fraction of myocytes positive for Ki67 (G) and phospho-H3 (H) increases with age more in women than men. F: female; M: male. \*p<0.05 vs. F. **I** and **J**, The rate of increase with age of amplifying myocytes positive for Ki67 (I) and mitotic myocytes positive phospho-H3 (J) is higher in the female than in the male LV.

**Figure 5. Aging and post-mitotic myocytes.** **A**, The fraction of young non-dividing myocytes decreases with age less in women than men. F: female; M: male. \*p<0.05 vs. F. **B**, The rate of decrease in the proportion of young non-dividing myocytes with age is lower in females than males.

**Figure 6. Aging, ploidy and cell fusion.** **A**, Frequency distribution of DNA content in young and old female and male cardiomyocytes. **B**, Fractions of diploid, tetraploid and octaploid myocyte nuclei. **C**, Example of myocytes in a female heart; myocyte nuclei carry at most two X-chromosomes (magenta dots). **D**, Male heart in which a dividing myocyte labeled by phospho-H3 (white) shows two sets of sex chromosomes (X-chromosome, magenta; Y-chromosome, green). The inset illustrates the organization of chromosomes in the dividing cell.

**Figure 7. Aging and myocyte formation.** **A**, Number of activated hCSCs. F: female; M: male. \*p<0.05 vs. F. **B**, Myocytes generated by a single hCSC. **C**, Number of divisions experienced by hCSCs before post-mitotic myocytes are formed. **D**, Number of post-mitotic myocytes generated by a single hCSC. **E**, The rate of myocyte formation with age is higher in the female than in the male myocardium. **F**, The degree of myocyte turnover with age is higher in the female than in the male myocardium.

**Figure 8. Organ aging and myocyte age.** **A**, The frequency distribution of myocyte age is shifted to the right in men. **B**, Frequency distribution of myocyte age in a woman 102 years old and a man 104 years old. Yellow area: myocytes younger than 2 years. Green area: myocytes older than 5.

**Figure 9. Organ aging and telomere length in hCSCs and myocytes.** **A-C**, Detection of telomeres by Q-FISH (white dots) in c-kit-positive hCSCs (green, arrows) and

cardiomyocytes in the young female (A) and in the young (B) and old (C) male heart. **D**, Telomere length in hCSCs and myocytes are shown individually and together in the four groups of hearts examined. F: female; M: male. \* $p < 0.05$  vs. F.

**Figure 10. Organ aging and myocyte senescence. A-C**, Myocyte precursors (c-kit, green;  $\alpha$ -SA, red) in the old female (A) and male (B and C) heart have telomeres shorter than 4kbp. **D**, The rate of acquisition of myocyte senescence becomes faster with age and it is slower in women than men.

## Online Supporting Information

### Legend to Figures

**Figure I. Aging and myocardial structure. A-F**, Minimal increases in interstitial fibrosis (collagen, yellow) are present in the left ventricle (LV) of old female and male hearts (A and B). Perivascular fibrosis (C and D) and foci of reparative fibrosis (E and F) are present in old female and male LV. Coronary arterioles are defined by  $\alpha$ -smooth muscle actin ( $\alpha$ -SMA, bright blue). **G-J**, Cardiomyocytes ( $\alpha$ -sarcomeric actin:  $\alpha$ -SA, red), defined by laminin (white), are similar in cross-sectional area in young female and male hearts (G and I). The increase in myocyte size with age is less apparent in the female than in the male LV (H and J). Age and gender are indicated in each panel. F: female; M: male; y: years.

**Figure II. Myocyte senescence and apoptosis. A-D**, The presence of p16<sup>INK4a</sup> (white) in myocyte nuclei is limited in the young female and male LV (A and C; arrows) and involves a larger number of cells in the old heart of both genders (B and D). Myocytes are stained by  $\alpha$ -SA (red). **E**, Emission spectra of p16<sup>INK4a</sup>-positive (green lines) and p16<sup>INK4a</sup>-negative (blue lines) myocyte nuclei. Inset: example of p16<sup>INK4a</sup>-labeled nuclei used for this analysis. Following normalization for fluorescence intensity, emission spectra of p16<sup>INK4a</sup>-positive myocyte nuclei are essentially superimposable, while emission spectra for tissue autofluorescence of p16<sup>INK4a</sup>-negative myocyte nuclei have a different shape. **F and G**, TUNEL (yellow) and p16<sup>INK4a</sup>-positive (white) myocyte nuclei (arrows) in the female (F) and male (G) LV. Insets illustrate separately TUNEL and p16<sup>INK4a</sup> labeling.

**Figure III. Myocyte progenitors and precursors. A-C**, Lineage negative hCSCs (arrowheads) are negative for transcription factors and cytoplasmic proteins (A and B). Myocyte progenitors (A, arrow) are c-kit-positive (green) and express GATA4 (white), myocyte precursors (B, arrow) are c-kit-positive and express Nkx2.5 (bright blue) and  $\alpha$ -SA (red), and amplifying myocytes (C, asterisk) are small cycling cells, positive for Ki67 (magenta) and lack c-kit. **D**, Emission spectra of c-kit, Nkx2.5, Ki67 and  $\alpha$ -SA positive (green lines) and negative (blue lines) cells. Examples of labeled nuclei and cells used for this analysis are shown in the insets. Following normalization for fluorescence intensity, emission spectra of c-kit, Nkx2.5, Ki67 and  $\alpha$ -SA positive cells are superimposable. The emission spectra for tissue autofluorescence have a different shape.

**Figure IV. Cycling hCSCs.** Small niches of Lin<sup>neg</sup>-c-kit<sup>pos</sup> hCSCs (green) containing Ki67 labeled cells (magenta, arrows).

**Figure V. Number of myocyte nuclei.** Percentage of mononucleated (Mo) and binucleated (Bi) myocytes in the young (19-49 years old) and old (72-104 years old) female and male heart.

**Figure VI. Aging and post-mitotic non-senescent and senescent myocytes.** In both women and men, the fraction of young non-dividing myocytes decreases with age, while the percentage of senescent p16<sup>INK4a</sup>-positive cells increases. These data were presented separately in Figures 3C and 5B.

**Figure VII. Aging and myocyte replacement based on the hierarchical model.** Myocyte turnover is higher in middle-age and old women than men. F: female; M: male. \*p<0.05 vs. F.

**Figure VIII. Organ age and average myocyte age based on the hierarchical model.** **A**, Younger myocytes are present in the female heart. F: female; M: male. \*p<0.05 vs. F. **B**, Inverse relationship between organ and myocyte age.

**Figure IX. Organ age and average myocyte age based on population dynamics model.** **A**, Younger myocytes are present in the female heart. F: female; M: male. \*p<0.05 vs. F. **B**, Inverse relationship between organ and myocyte age.

**Figure X. Aging and myocyte replacement based on population dynamics model.** **A**, Myocyte turnover is higher in middle-age and old women than men. F: female; M: male. \*p<0.05 vs. F. **B**, The rate of myocyte turnover with age is higher in the female than in the male myocardium.

**Figure XI. Telomere length in hCSCs and myocytes.** Frequency distribution of telomere length in hCSCs and cardiomyocytes. Yellow area: nuclei with telomeres equal and longer than 8kbp.

**Table I. Inclusion Criteria.**

**Table II. Patients and Cardiac Characteristics**

**Table III. Magnitude of Sampling**

**Table IV. Immunolabeling**

**Scheme I. Exponential Cell Growth**

This scheme shows that division of one hCSC may lead to the formation of 256 myocytes by 8 consecutive divisions. The first gives rise to 2 progenitors, the second to 4 precursors and the third to 8 amplifying myocytes; if these cells divide 5 times, 256 mature myocytes are formed.

**Scheme II. Transit Generations of hCSCs**

Gt reflects the number of divisions that 1 hCSC goes through before differentiation is acquired. For example, with 1 transit generation (1 Gt), 2 mature cells are formed and with 3 Gt, 8 mature cells are created.

**Material and Methods**

## **Patients**

Seventy-four hearts, 32 female and 42 male, collected from individuals who died from causes other than cardiovascular diseases and met the criteria listed in Table I were studied. Patients' characteristics, cause of death, and the anatomical properties of the heart are indicated in Table II. Only samples of the left ventricle, fixed in formalin and embedded in paraffin, were studied. The degree of sampling for each quantitative parameter is shown in Table III. For each measurement, aggregate sampling error was maintained consistently below 10% which is significantly lower than the biological variability among patients.<sup>1</sup>

## **Immunocytochemistry**

Tissue sections, 4  $\mu\text{m}$  thick, were subjected to antigen-retrieval protocols and labeled with specific antibodies. Antibodies were directly labeled with fluorochromes or quantum dots to avoid cross-reactivity and autofluorescence. Antigens, antibodies and the methodology of detection of individual proteins<sup>2-7</sup> are listed in Table IV. Y- and X-chromosomes were identified by FISH with human specific probes.<sup>3,4,8</sup> The specificity of the recorded signals was confirmed by spectral analysis.<sup>9,10</sup>

## **Spectral Analysis**

This technique was performed with a Zeiss LSM510 Meta confocal microscope (Zeiss) utilizing the meta detector and the lambda acquisition mode. The emission signal for each epitope was excited at 405, 488, 543 and 633 nm with an argon laser and its fluorescence intensity was recorded generating a lambda stack ranging from 427 to 748 nm at 10.7 nm intervals. The lens and corresponding numerical aperture were 60X and 1.4, respectively. For each region of interest, a graph plotting mean pixel intensity and the emission wavelength of the lambda stack was generated. To compare the shape of each curve, the values of emission spectra were normalized by dividing the intensity of each wavelength by the peak signal. The spectrum obtained from each actual signal exhibited a well-defined peak while the spectrum of autofluorescence was spread across the range of wavelengths and did not show a clearly defined peak.<sup>9,10</sup>

## **hCSCs and their Progeny**

Lineage negative c-kit-positive hCSCs and early committed cells were identified and measured quantitatively by mixtures of antibodies labeled directly with fluorochromes (Table IV). The epitopes employed to classify hCSCs, myocyte progenitors, myocyte precursors and amplifying myocytes are listed in Table IV. This analysis was based on procedures previously employed in our laboratory.<sup>11,12</sup> Additionally, the fraction of cycling hCSCs and amplifying myocytes and their mitotic index were defined by Ki67 and phospho-H3 labeling. Cytokinesis was detected by aurora B kinase.

## **Length of the Cell Cycle in hCSCs**

An additional set of experiments concerning the function of hCSCs involved the in vitro evaluation of the duration of their cell cycle. Only FACS sorted lineage negative c-kit-positive hCSCs were employed. These hCSCs were obtained from the right atrial appendage of 4 patients, 2 men (age: 56 and 83 years) and 2 women (age: 50 and 72 years), who underwent coronary bypass surgery. hCSCs were pulse-labeled with BrdU for 20 min and cells were fixed at one hour intervals up to 48 hours<sup>13</sup> to assess the percentage of labeled mitosis. This parameter was derived from a total of 1,041 hCSCs in mitosis and plotted as a function of time.

The length of G2 (TG2) was equal to the time elapsed between the removal of BrdU and the presence of BrdU in 50% mitotic hCSCs. The length of S-phase (TS) corresponded to the interval between the first ascending limb and the first descending limb of the labeled mitotic curve. Moreover, the length of G1 (TG1) was given by the interval between the first descending limb and the second ascending limb of the curve. Using time-lapse recording, the duration of mitosis (TM) was assessed. Thus, the length of cell cycle, TC, was calculated as follows:  $TC = TG1 + TS + TG2 + TM$ .

### **Post-Mitotic Myocytes and Senescent Myocytes**

Young, terminally-differentiated myocytes were identified by the absence of Ki67<sup>14</sup> and p16<sup>INK4a</sup><sup>11,15,16</sup>. Old, terminally-differentiated myocytes were recognized by the nuclear localization of p16<sup>INK4a</sup>. The number of these two cell populations in the myocardium was measured by a quantitative methodology developed and repeatedly employed in our laboratory.<sup>1,17-20</sup> Similarly, the proportion of mononucleated and binucleated myocytes was assessed by staining the junctional protein connexin 43 in 10-12  $\mu$ m thick tissue sections. Additionally, myocyte apoptosis was evaluated quantitatively by the TdT assay.<sup>21</sup>

### **DNA Content in Myocyte Nuclei**

Myocyte nuclei were labeled with propidium iodide and the intensity of the DNA signal in each nucleus was measured by confocal microscopy and ImagePro software. Only nuclei which were completely included in the thickness of the section were considered for this analysis. Lymphocytes present in sections of human tonsils were used as control for diploid  $2n$  values. Samples were also stained with Ki67 to distinguish cycling and non-cycling cells.<sup>4,22</sup>

### **Telomere Length in Myocytes and hCSCs**

Telomere length in hCSC and myocyte nuclei was evaluated in tissue sections by quantitative fluorescence in situ hybridization (Q-FISH) and confocal microscopy, using a peptide nucleic acid probe labeled by FITC.<sup>3,11</sup> The fluorescent signals measured in lymphoma cells (L5178Y) with short (7 kbp) and long (48 kbp) telomeres (kindly provided by Dr. M.A. Blasco, Madrid, Spain) were utilized to compute absolute telomere length. Individual telomere signals in each nucleus were added and divided by the DAPI signal to correct for differences in the nuclear fraction included in the section.

### **Origin and Rate of Myocyte Formation**

To establish the kinetics of hCSCs and myocytes in the aging heart, a hierarchically structured cell system was applied.<sup>12,23</sup> This mathematical model is based on the analysis of individual cells within the tissue. This information is then translated into the history of the cell or its fate. A myocardial section is composed of hCSCs and different proportions of myocyte progenitors, precursors, transit amplifying myocytes and terminally-differentiated cells. The number of each cell class was measured (see above) and their relative contribution defined. The number of divisions required for each cell category to generate the progeny present in the next hierarchical level was also derived. For example, division of one hCSC may lead to the formation of 256 myocytes by 8 consecutive divisions (Scheme I). The required primary data included the number of hCSCs, LCCs, (lineage committed cells: myocyte progenitors and precursors), and the number of myocytes per 10 g of myocardium ( $V$ ). Also, the fraction of cycling hCSCs was determined together with the length of their cell cycle.

According to the hierarchical model of cell growth and differentiation,<sup>23</sup> the rate of entry (Rs) of hCSCs into the cell cycle was given by  $R_s = f \times (N_s/T_s)$  where  $N_s$  is the number of hCSCs per V,  $T_s$  is the length of their cell cycle, and  $f$  the percentage of cycling hCSCs. The rate of generation of differentiated myocytes,  $r$ , was derived from:  $r = ((f \times N_s)/T_s) \times 2^{G_t}$  where the exponent  $G_t$  equals the number of transit generations, i.e., the number of divisions that one LCC will go through before it loses c-kit and acquires the properties of amplifying myocytes (Scheme II).  $G_t$  was derived from the ratio of LCCs and hCSCs. Following division of one hCSC, the daughter cell destined to become a myocyte generated two LCCs. Thus, if one generation is in transit, 2 LCCs are present for each hCSC. If 2 generations are in transit, 4 LCCs are found for each hCSC. For  $n$  generations in transit,  $2^n$  LCCs are detected:  $N_c = N_s \times 2^{G_t}$ , where  $N_s$  and  $N_c$  represent the number of hCSCs and LCCs per V, respectively.  $G_t$  was calculated from:  $G_t = \log(N_c/N_s) / \log 2$ .  $G_t$  was then substituted so that:  $r = ((f \times N_s)/T_s) \times 2^{(\log(N_c/N_s) / \log 2)}$ . This equation was used to measure the birth rate of hCSC-derived myocytes in each heart.

### Age Distribution of Cardiomyocytes

This parameter was obtained utilizing the data on cycling and mitotic myocytes in combination with the values of myocyte death. These variables were employed to define the ages of myocytes at any time in life. The mathematical model used is based on the differential McKendrick-von Foerster equation developed originally to assess aging and death of all species in their environment.<sup>24</sup> This approach is equally valid for the measurement of age and death of age-structured cell populations.<sup>25</sup>

The original McKendrick-von Foerster equation reads  $(\partial n(a,t)) / \partial t = - (\partial n(a,t)) / \partial a - \mu(a,t) \times n(a,t)$ . Specifically, the function  $n(a,t)$  defines the number of cells of age  $a$  in a subject of age  $t$ ; the derivative function  $(\partial n(a,t)) / \partial t$  characterizes the rate of cell generation within the population; the derivative function  $(\partial n(a,t)) / \partial a$  describes the proportion of cells of different ages within the population; and the function  $\mu(a,t)$  identifies the mortality rate of cells with age  $a$  at time  $t$ . Since our data document that myocyte age is shorter than individual age, we assume that the fraction of cells of age  $a$  is a variable independent from patient's age  $t$ . Thus, the equation was changed to:  $(\partial n(a)) / \partial t = - (\partial n(a)) / \partial a - \mu(a,t) \times n(a)$ . Additionally,  $\partial n(a) / \partial t \approx 0$  so that  $n(a) = (\partial n(a)) / \partial a / \mu(a,t)$ . The function  $\mu(a,t)$  reflected the measured age-dependent levels of myocyte death. Assuming a Gaussian distribution of myocyte age,  $[(\partial n(a)) / \partial a]$  was substituted by  $N \times e^{-[(a^2) / (2 \times h^2)]}$  in which  $N$  is the number of myocytes per 10 g of myocardium (V) and  $h$  represents their half-life time. Thus, at any given age, the number of myocytes with age  $a$  was given by  $n(a) = N \times e^{-[(a^2) / (2 \times h^2)]} / (\mu(a,t))$ .

### Statistical Analysis

Results are presented as mean $\pm$ SD. Differences between women and men in each age group were determined by two-tailed unpaired Student's  $t$  test. Differences among groups were established by the analysis of variance and the Bonferroni method. Linear regressions were calculated by the least squares method. Comparisons between slopes were made by the analysis of covariance.<sup>26</sup>

### References

1. Anversa P, Olivetti G. Cellular basis of physiological and pathological myocardial growth. In: Page E, Fozzard HA, Solaro RJ, editors. Handbook of Physiology: The Cardiovascular System: The Heart. Oxford University Press. 2002; pp. 75-144.

2. Anversa P, Leri A, Rota M, Hosoda T, Bearzi C, Urbanek K, Kajstura J, Bolli R. Concise review: stem cells, myocardial regeneration, and methodological artifacts. *Stem Cells*. 2007;25:589-601.
3. Rota M, Kajstura J, Hosoda T, Bearzi C, Vitale S, Esposito G, Iaffaldano G, Padin-Iruegas ME, Gonzalez A, Rizzi R, Small N, Muraski J, Alvarez R, Chen X, Urbanek K, Bolli R, Houser SR, Leri A, Sussman MA, Anversa P. Bone marrow cells adopt the cardiomyogenic fate in vivo. *Proc Natl Acad Sci USA*. 2007;104:17783-17788.
4. Bearzi C, Rota M, Hosoda T, Tillmanns J, Nascimbene A, De Angelis A, Yasuzawa-Amano S, Trofimova I, Siggins RW, Lecapitaine N, Cascapera S, Beltrami AP, D'Alessandro DA, Zias E, Quaini F, Urbanek K, Michler RE, Bolli R, Kajstura J, Leri A, Anversa P. Human cardiac stem cells. *Proc Natl Acad Sci USA*. 2007;104:14068-14073.
5. Rota M, Padin-Iruegas ME, Misao Y, De Angelis A, Maestroni S, Ferreira-Martins J, Fiumana E, Rastaldo R, Arcarese ML, Mitchell TS, Boni A, Bolli R, Urbanek K, Hosoda T, Anversa P, Leri A, Kajstura J. Local activation or implantation of cardiac progenitor cells rescues scarred infarcted myocardium improving cardiac function. *Circ Res*. 2008;103:107-116.
6. Padin-Iruegas ME, Misao Y, Davis ME, Segers VF, Esposito G, Tokunou T, Urbanek K, Hosoda T, Rota M, Anversa P, Leri A, Lee RT, Kajstura J. Cardiac progenitor cells and biotinylated insulin-like growth factor-1 nanofibers improve endogenous and exogenous myocardial regeneration after infarction. *Circulation*. 2009;120:876-887.
7. Bearzi C, Leri A, Lo Monaco F, Rota M, Gonzalez A, Hosoda T, Pepe M, Qanud K, Ojaimi C, Bardelli S, D'Amario D, D'Alessandro DA, Michler RE, Dimmeler S, Zeiher AM, Urbanek K, Hintze TH, Kajstura J, Anversa P. Identification of a coronary vascular progenitor cell in the human heart. *Proc Natl Acad Sci USA*. 2009;106:15885-15890.
8. Quaini F, Urbanek K, Beltrami AP, Finato N, Beltrami CA, Nadal-Ginard B, Kajstura J, Leri A, Anversa P. Chimerism of the transplanted heart. *N Engl J Med*. 2002;346:5-15.
9. Hosoda T, D'Amario D, Cabral-Da-Silva MC, Zheng H, Padin-Iruegas ME, Ogorek B, Ferreira-Martins J, Yasuzawa-Amano S, Amano K, Ide-Iwata N, Cheng W, Rota M, Urbanek K, Kajstura J, Anversa P, Leri A. Clonality of mouse and human cardiomyogenesis in vivo. *Proc Natl Acad Sci USA*. 2009;106:17169-17174.
10. D'Alessandro DA, Kajstura J, Hosoda T, Gatti A, Bello R, Mosna F, Bardelli S, Zheng H, D'Amario D, Padin-Iruegas ME, Carvalho AB, Rota M, Zembala MO, Stern D, Rimoldi O, Urbanek K, Michler RE, Leri A, Anversa P. Progenitor cells from the explanted heart generate immunocompatible myocardium within the transplanted donor heart. *Circ Res*. 2009;105:1128-1140.
11. Urbanek K, Torella D, Sheikh F, De Angelis A, Nurzynska D, Silvestri F, Beltrami CA, Bussani R, Beltrami AP, Quaini F, Bolli R, Leri A, Kajstura J, Anversa P. Myocardial regeneration by activation of multipotent cardiac stem cells in ischemic heart failure. *Proc Natl Acad Sci USA*. 2005;102:8692-8697.
12. Urbanek K, Cesselli D, Rota M, Nascimbene A, De Angelis A, Hosoda T, Bearzi C, Boni A, Bolli R, Kajstura J, Anversa P, Leri A. Stem cell niches in the adult mouse heart. *Proc Natl Acad Sci USA*. 2006;103:9226-9231.
13. Baserga R. The cell cycle. In: Baserga R, ed. *The Biology of Cell Reproduction*. Cambridge, Mass: Harvard University Press; 1985:3-21.

14. Scholzen T, Gerdes J. The Ki-67 protein: from the known and the unknown. *J Cell Physiol.* 2000;182:311-322.
15. Chimenti C, Kajstura J, Torella D, Urbanek K, Heleniak H, Colussi C, Di Meglio F, Nadal-Ginard B, Frustaci A, Leri A, Maseri A, Anversa P. Senescence and death of primitive cells and myocytes lead to premature cardiac aging and heart failure. *Circ Res.* 2003;93:604-613.
16. Beausejour CM, Campisi J. Ageing: balancing regeneration and cancer. *Nature.* 2006;443:404-405.
17. Beltrami CA, Finato N, Rocco M, Feruglio GA, Puricelli C, Cigola E, Quaini F, Sonnenblick EH, Olivetti G, Anversa P. Structural basis of end-stage failure in ischemic cardiomyopathy in humans. *Circulation.* 1994;89:151-163.
18. Olivetti G, Melissari M, Balbi T, Quaini F, Sonnenblick EH, Anversa P. Myocyte nuclear and possible cellular hyperplasia contribute to ventricular remodeling in the hypertrophic senescent heart in humans. *J Am Coll Cardiol.* 1994;24:140-149.
19. Beltrami CA, Finato N, Rocco M, Feruglio GA, Puricelli C, Cigola E, Sonnenblick EH, Olivetti G, Anversa P. The cellular basis of dilated cardiomyopathy in humans. *J Mol Cell Cardiol.* 1995;27:291-305.
20. Olivetti G, Giordano G, Corradi D, Melissari M, Lagrasta C, Gambert SR, Anversa P. Gender differences and aging: effects on the human heart. *J Am Coll Cardiol.* 1995;26:1068-1079.
21. Olivetti G, Abbi R, Quaini F, Kajstura J, Cheng W, Nitahara JA, Quaini E, Di Loreto C, Beltrami CA, Krajewski S, Reed JC, Anversa P. Apoptosis in the failing human heart. *N Engl J Med.* 1997;336:1131-1141.
22. Beltrami AP, Barlucchi L, Torella D, Baker M, Limana F, Chimenti S, Kasahara H, Rota M, Musso E, Urbanek K, Leri A, Kajstura J, Nadal-Ginard B, Anversa P. Adult cardiac stem cells are multipotent and support myocardial regeneration. *Cell.* 2003;114:763-776.
23. Savill NJ. Mathematical models of hierarchically structured cell populations under equilibrium with application to the epidermis. *Cell Prolif.* 2003;36:1-26.
24. Milner FA, Rabbio G. Rapidly converging numerical algorithms for models of population dynamics. *J Math Biol.* 30: 733-753.
25. Logan JD, Ledder G, Wolessky W. Type II functional response for continuous, physiologically structured models. *J Theor Biol.* 2009;259:373-381.
26. Berenson ML, Levine DM, Rindskopf D. Simple linear regression and correlation. In: Berenson ML, Levine DM, Rindskopf D, eds. *Applied Statistics*. Englewood Cliffs, NJ: Prentice Hall; 1998:362-418.

## **Table I. Inclusion Criteria**

---

### **Clinical Criteria**

1. Sudden death associated with traumatic injury
2. Death within 5 days of hospitalization in the absence of cardiovascular disease
3. Absence of hypertension, diabetes or ischemic heart disease
4. Body weight within 20% of optimal weight according to sex, height and age
5. Lack of clinically recognized systemic disorders

### **Anatomical Criteria**

1. Lack of atherosclerosis of major coronary arteries or reduction of luminal diameter <30%
2. Lack of acute or healed myocardial infarction
3. Heart weight <500g
4. Absence of diffuse emphysema and chronic inflammation of the respiratory system
5. Lack of malignant neoplasm with multiple metastatic localizations

### **Histological Criteria**

1. Absence of neoplasms of the hematopoietic system
  2. Lack of amyloidosis, tuberculosis and sarcoidosis
  3. Negative for diffuse interstitial and perivascular fibrosis
  4. Lack of thickening and hyalinosis of the intermediate-sized coronary vessels
  5. Absence of foci of replacement fibrosis or presence of lesions <2 mm in diameter
  6. Lack of inflammation of the myocardial interstitium
  7. Absence of myocytolytic and contraction band necrosis
-

**Table II. Patients and Cardiac Characteristics**

| Age (years) | Gender | Body Weight (kg) | Height (cm) | Body Mass Index (kg/m <sup>2</sup> ) | Heart Weight (g) | LV Weight (g) | Cause of Death            |
|-------------|--------|------------------|-------------|--------------------------------------|------------------|---------------|---------------------------|
| 104         | M      | 70               | 170         | 24.2                                 | 265              | 195           | pneumonia                 |
| 102         | F      | 50               | 150         | 22.2                                 | 240              | 180           | cerebral aneurism         |
| 99          | F      | 45               | 145         | 21.4                                 | 187              | 139           | pulmonary thromboembolism |
| 98          | M      | 50               | 170         | 17.3                                 | 215              | 165           | gastric adenocarcinoma    |
| 98          | F      | 65               | 173         | 21.7                                 | 234              | 175           | cerebral aneurism         |
| 96          | F      | 50               | 160         | 19.6                                 | 200              | 150           | pulmonary thromboembolism |
| 94          | F      | 40               | 150         | 17.8                                 | 200              | 148           | pneumonia                 |
| 93          | M      | 75               | 175         | 24.5                                 | 325              | 250           | pulmonary thromboembolism |
| 93          | F      | 40               | 165         | 14.7                                 | 175              | 130           | intestinal occlusion      |
| 92          | F      | 52               | 152         | 21.6                                 | 201              | 150           | abdominal aorta aneurism  |
| 91          | F      | 50               | 155         | 20.8                                 | 240              | 175           | pulmonary thromboembolism |
| 91          | F      | 40               | 150         | 17.8                                 | 220              | 160           | aortic aneurism           |
| 91          | F      | 40               | 150         | 17.8                                 | 155              | 115           | pulmonary thromboembolism |
| 90          | M      | 60               | 170         | 20.8                                 | 290              | 225           | pulmonary thromboembolism |
| 90          | M      | 70               | 160         | 27.3                                 | 205              | 155           | pulmonary thromboembolism |
| 89          | M      | 60               | 180         | 18.5                                 | 350              | 245           | pneumonia                 |
| 89          | F      | 63               | 165         | 23.3                                 | 200              | 148           | cerebral aneurism         |
| 86          | F      | 70               | 160         | 27.3                                 | 340              | 255           | pneumonia                 |
| 79          | M      | 66               | 164         | 24.5                                 | 194              | 151           | aortic aneurism           |
| 77          | F      | 62               | 155         | 25.8                                 | 174              | 135           | pneumonia                 |
| 75          | F      | 60               | 153         | 25.6                                 | 166              | 129           | pneumonia                 |
| 74          | M      | 65               | 165         | 23.9                                 | 247              | 192           | pulmonary thromboembolism |
| 74          | M      | 65               | 165         | 23.9                                 | 290              | 220           | pneumonia                 |
| 74          | F      | 72               | 174         | 23.8                                 | 267              | 204           | cerebral aneurism         |
| 73          | M      | 67               | 168         | 23.7                                 | 236              | 174           | cerebral aneurism         |
| 72          | M      | 70               | 168         | 24.8                                 | 212              | 156           | pneumonia                 |
| 71          | F      | 64               | 165         | 23.5                                 | 188              | 138           | acute trauma              |

|    |   |    |     |      |     |     |                              |
|----|---|----|-----|------|-----|-----|------------------------------|
| 69 | M | 85 | 185 | 24.8 | 230 | 175 | pulmonary embolism           |
| 69 | M | 55 | 165 | 22.9 | 250 | 210 | pneumonia                    |
| 69 | M | 60 | 170 | 20.8 | 240 | 180 | pneumonia                    |
| 69 | F | 70 | 170 | 24.2 | 215 | 165 | pulmonary artery embolism    |
| 68 | M | 50 | 165 | 18.4 | 240 | 180 | acute distress resp. syndrom |
| 68 | M | 62 | 160 | 24.2 | 243 | 189 | pneumonia                    |
| 67 | F | 65 | 170 | 22.5 | 240 | 180 | pneumonia                    |
| 66 | F | 55 | 165 | 20.2 | 315 | 240 | abdominal aortic aneurism    |
| 66 | F | 70 | 160 | 27.3 | 280 | 210 | aortic dissection            |
| 62 | F | 67 | 155 | 27.9 | 270 | 210 | pneumonia                    |
| 60 | M | 70 | 185 | 20.5 | 290 | 230 | pneumonia                    |
| 60 | M | 60 | 175 | 19.6 | 180 | 140 | pneumonia                    |
| 60 | M | 75 | 180 | 23.1 | 355 | 280 | pneumonia                    |
| 60 | M | 50 | 160 | 19.5 | 255 | 190 | gastrointestinal hemorrhage  |
| 60 | F | 53 | 158 | 21.2 | 178 | 131 | acute trauma                 |
| 59 | F | 55 | 175 | 18.0 | 225 | 170 | pneumonia                    |
| 58 | M | 60 | 160 | 23.4 | 330 | 270 | pneumonia                    |
| 57 | F | 80 | 170 | 27.7 | 310 | 240 | acute hemorrh. pancreatitis  |
| 56 | M | 85 | 186 | 24.6 | 240 | 180 | pneumonia                    |
| 55 | M | 76 | 170 | 26.3 | 180 | 135 | pneumonia                    |
| 54 | M | 85 | 175 | 27.8 | 200 | 150 | pneumonia                    |
| 52 | F | 55 | 155 | 22.9 | 174 | 140 | acute hemorrhage             |
| 51 | F | 62 | 163 | 23.3 | 250 | 184 | pneumonia                    |
| 50 | M | 70 | 185 | 20.5 | 230 | 180 | pneumonia                    |
| 50 | F | 76 | 165 | 27.9 | 185 | 150 | hemorrhagic ictus            |
| 49 | M | 70 | 169 | 24.5 | 210 | 160 | cerebral stroke              |
| 49 | M | 73 | 174 | 24.1 | 219 | 169 | suicide                      |
| 48 | M | 68 | 175 | 22.2 | 310 | 235 | pneumonia                    |
| 45 | F | 58 | 156 | 23.8 | 161 | 124 | acute trauma                 |
| 44 | M | 70 | 180 | 21.6 | 175 | 130 | aortic rupture               |
| 42 | F | 59 | 165 | 21.7 | 170 | 130 | abdominal aortic aneurism    |
| 42 | F | 53 | 160 | 20.7 | 170 | 115 | pneumonia                    |
| 41 | F | 40 | 130 | 23.7 | 190 | 140 | multiorgan failure           |
| 41 | F | 63 | 165 | 23.1 | 180 | 140 | cerebral aneurism            |

|    |   |     |     |      |     |     |                             |
|----|---|-----|-----|------|-----|-----|-----------------------------|
| 39 | F | 63  | 176 | 20.3 | 220 | 174 | cerebral aneurism           |
| 38 | F | 52  | 160 | 20.3 | 250 | 210 | acute trauma                |
| 35 | M | 75  | 188 | 21.2 | 261 | 201 | acute trauma                |
| 34 | M | 90  | 180 | 27.8 | 275 | 206 | gastrointestinal hemorrhage |
| 34 | F | 63  | 158 | 25.2 | 205 | 158 | pneumonia                   |
| 33 | M | 90  | 180 | 27.8 | 270 | 215 | craniopharyngioma           |
| 32 | M | 75  | 180 | 23.1 | 194 | 143 | acute trauma                |
| 32 | M | 70  | 175 | 22.9 | 215 | 160 | suicide                     |
| 31 | M | 75  | 165 | 27.5 | 280 | 205 | acute trauma                |
| 31 | M | 80  | 170 | 27.7 | 320 | 240 | abdominal aortic aneurism   |
| 30 | M | 65  | 177 | 20.7 | 200 | 150 | suicide                     |
| 29 | M | 80  | 187 | 22.9 | 215 | 160 | acute trauma                |
| 28 | M | 100 | 190 | 27.7 | 360 | 210 | thoracic aortic aneurism    |
| 26 | F | 53  | 158 | 21.2 | 192 | 142 | pneumonia                   |
| 24 | M | 70  | 177 | 22.3 | 270 | 200 | acute trauma                |
| 23 | M | 80  | 195 | 21.0 | 390 | 300 | acute trauma                |
| 21 | F | 50  | 165 | 18.4 | 210 | 170 | acute trauma                |
| 20 | M | 81  | 183 | 24.2 | 193 | 149 | acute trauma                |
| 19 | M | 70  | 185 | 20.5 | 340 | 300 | cerebral aneurism           |

---

Heart weight was determined following removal of epicardial fat.

**Table III.** Magnitude of Sampling

| Parameter                                      | Aggregate sample size    | Sample size (mean ± SD) | Sampling Error |
|--|--------------------------|-------------------------|----------------|
| p16 <sup>INK4a</sup> -positive Myocytes        |                          |                         |                |
| Females  | 8,817 <sup>(1)</sup>     | 275±99                  | 6.0%           |
| Males  | 10,785 <sup>(1)</sup>    | 257±128                 | 6.2%           |
| Apoptotic Myocytes                             |                          |                         |                |
| Females  | 2,449,600 <sup>(1)</sup> | 76,550±35,064           | 6.3%           |
| Males  | 2,883,825 <sup>(1)</sup> | 68,663±27,781           | 5.8%           |
| Lin <sup>neg</sup> -c-kit <sup>pos</sup> hCSCs |                          |                         |                |
| Females  | 8,267 <sup>(2)</sup>     | 258±84                  | 4.4%           |
| Males  | 12,349 <sup>(2)</sup>    | 294±97                  | 4.3%           |
| Proliferating hCSCs                            |                          |                         |                |
| Females  | 994 <sup>(1)</sup>       | 31.1±7.8                | 3.2%           |
| Males  | 1,143 <sup>(1)</sup>     | 27.2±6.8                | 3.0%           |
| Senescent hCSCs                                |                          |                         |                |
| Females  | 9,409 <sup>(1)</sup>     | 294±128                 | 1.0%           |
| Males  | 9,957 <sup>(1)</sup>     | 237±74                  | 1.0%           |
| Myocyte Progenitors and Precursors             |                          |                         |                |
| Females  | 8,895 <sup>(1)</sup>     | 278±121                 | 1.0%           |
| Males  | 9,402 <sup>(1)</sup>     | 224±70                  | 1.0%           |
| Amplifying Myocytes                            |                          |                         |                |
| Females  | 1,380,225 <sup>(1)</sup> | 34,500±6,517            | 0.5%           |
| Males  | 1,449,000 <sup>(1)</sup> | 32,863±7,215            | 0.5%           |
| Mitotic Myocytes                               |                          |                         |                |
| Females  | 2,706,900 <sup>(1)</sup> | 64,450±9,947            | 0.4%           |
| Males  | 3,037,020 <sup>(1)</sup> | 72,310±10,691           | 0.4%           |
| DNA Content in Myocytes                        |                          |                         |                |
| Females  | 2,035 <sup>(1)</sup>     | 204±9                   | 6.9%           |
| Males  | 2,089 <sup>(1)</sup>     | 209±10                  | 7.0%           |
| Number of Nuclei in Myocytes                   |                          |                         |                |
| Females  | 4,441 <sup>(1)</sup>     | 444±42                  | 4.7%           |
| Males  | 4,384 <sup>(1)</sup>     | 438±28                  | 4.8%           |
| FISH for Sex Chromosomes in Myocytes           |                          |                         |                |
| Females  | 3,418 <sup>(1)</sup>     | 342±53                  | 5.4%           |
| Males  | 3,261 <sup>(1)</sup>     | 326±60                  | 5.5%           |

|                             |                      |        |      |
|-----------------------------|----------------------|--------|------|
| Telomere Length in CSCs     |                      |        |      |
| Females                     | 264 <sup>(1)</sup>   | 26±3   | 6.2% |
| Males                       | 276 <sup>(1)</sup>   | 28±3   | 6.0% |
| Telomere Length in Myocytes |                      |        |      |
| Females                     | 1,192 <sup>(1)</sup> | 119±8  | 2.9% |
| Males                       | 1,120 <sup>(1)</sup> | 112±12 | 3.0% |

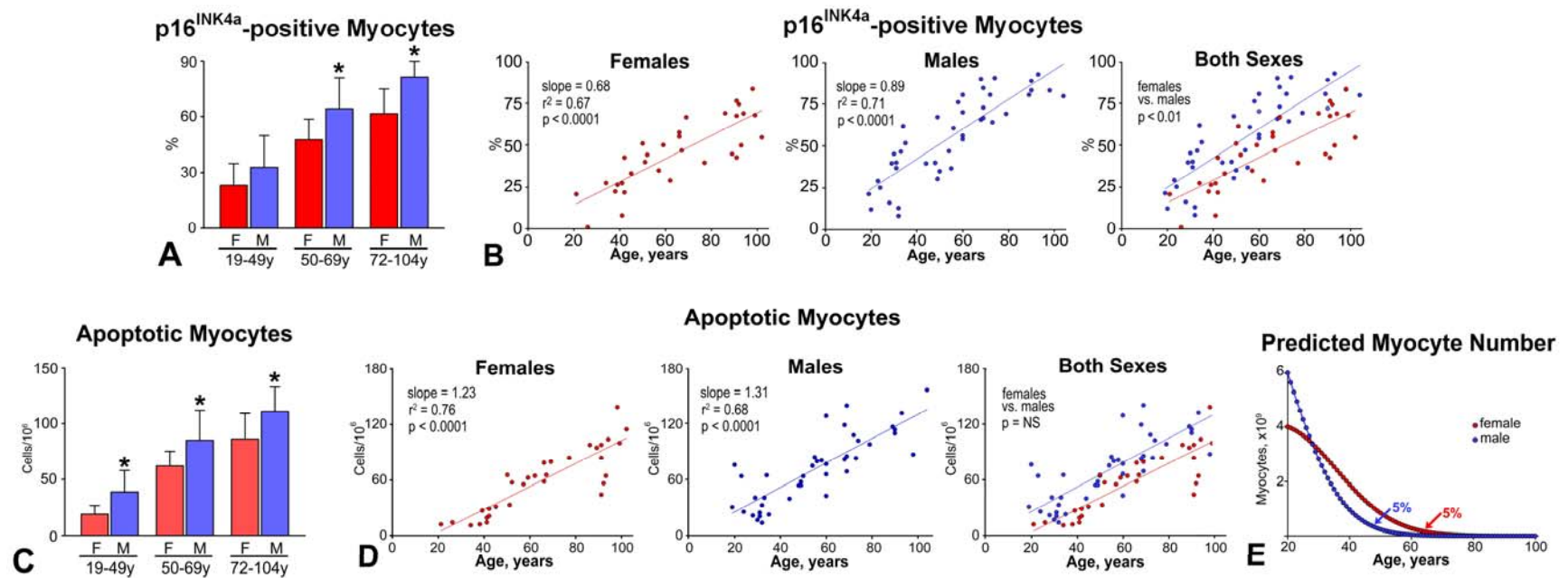
---

<sup>(1)</sup> Total number of nuclei analyzed; <sup>(2)</sup> Area of myocardium analyzed to establish the number of Lin<sup>neg</sup>-c-kit<sup>pos</sup> hCSCs.

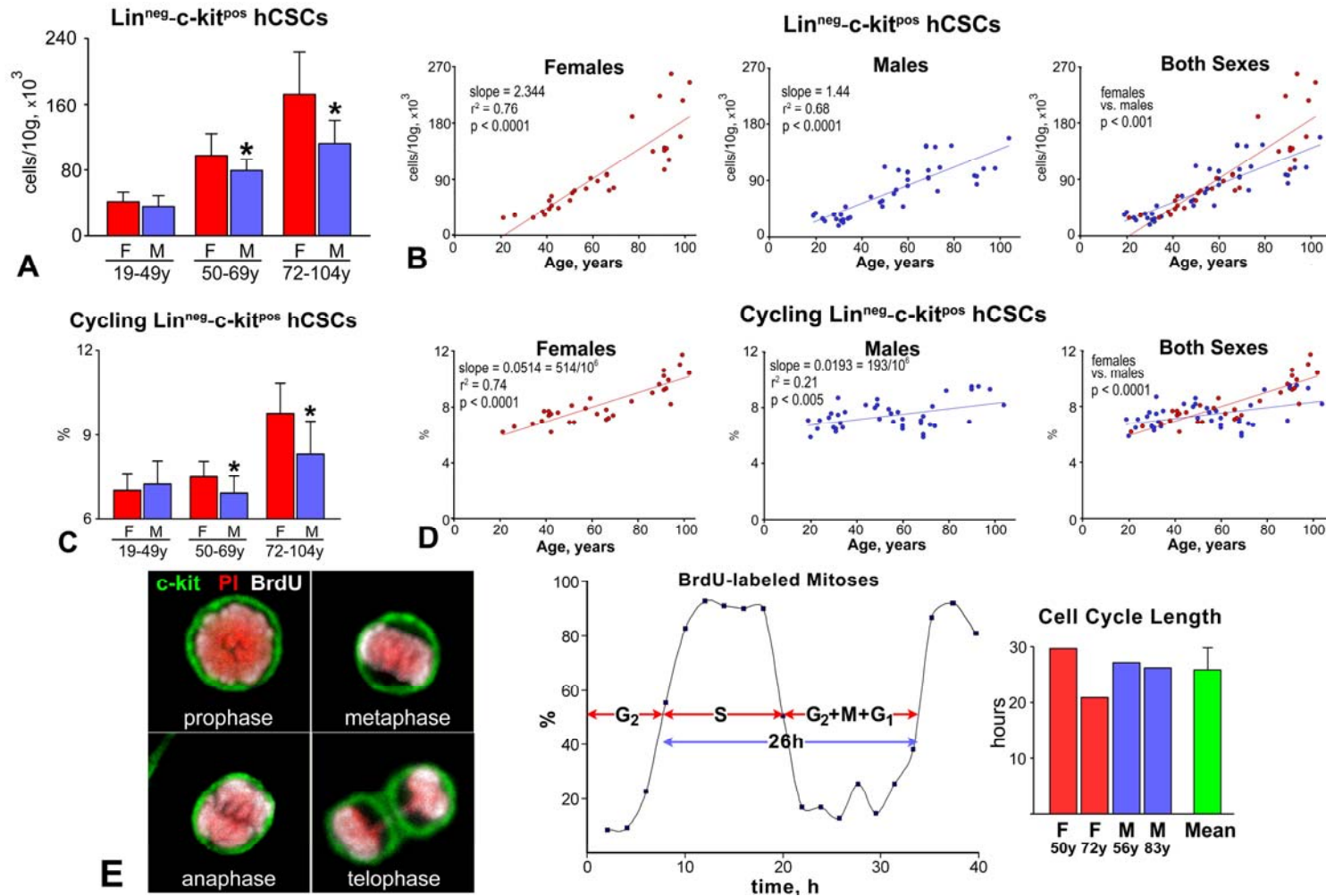
**Table IV.** Immunolabeling

| Protein                    | Antibody          | Labeling            | Fluorochromes    |
|----------------------------|-------------------|---------------------|------------------|
| c-kit                      | rabbit polyclonal | direct and indirect | F, T, QD655      |
| GATA4                      | rabbit polyclonal | indirect            | T, Cy5           |
| Nkx2.5                     | goat polyclonal   | indirect            | F, T, Cy5        |
| $\alpha$ -sarcomeric actin | mouse monoclonal  | direct              | F, T, Cy5, QD655 |
| $\alpha$ -smooth actin     | mouse monoclonal  | direct              | T, Cy5, QD655    |
| Ki67                       | rabbit polyclonal | indirect            | F, T, Cy5        |
| Phospho-H3                 | mouse monoclonal  | direct, indirect    | T, Cy5, QD655    |
| Aurora B kinase            | rabbit polyclonal | indirect            | T, Cy5           |
| p16 <sup>INK4a</sup>       | goat polyclonal   | indirect            | F, T, Cy5        |
| Nuclear DNA                | DAPI, PI          | N/A                 | N/A              |
| X and Y chromosomes        | DNA probe         | direct              | F, Cy3           |
| TUNEL                      | TdT/dUTP          | direct              | F, T             |

Direct labeling: primary antibody conjugated with the fluorochrome. Indirect labeling: species-specific secondary antibody conjugated with the fluorochrome. F: fluorescein isothiocyanate, T: tetramethyl rhodamine isothiocyanate, Cy3: cyanine 3, Cy5: cyanine 5, QD655: quantum dots with emission at 655 nm.

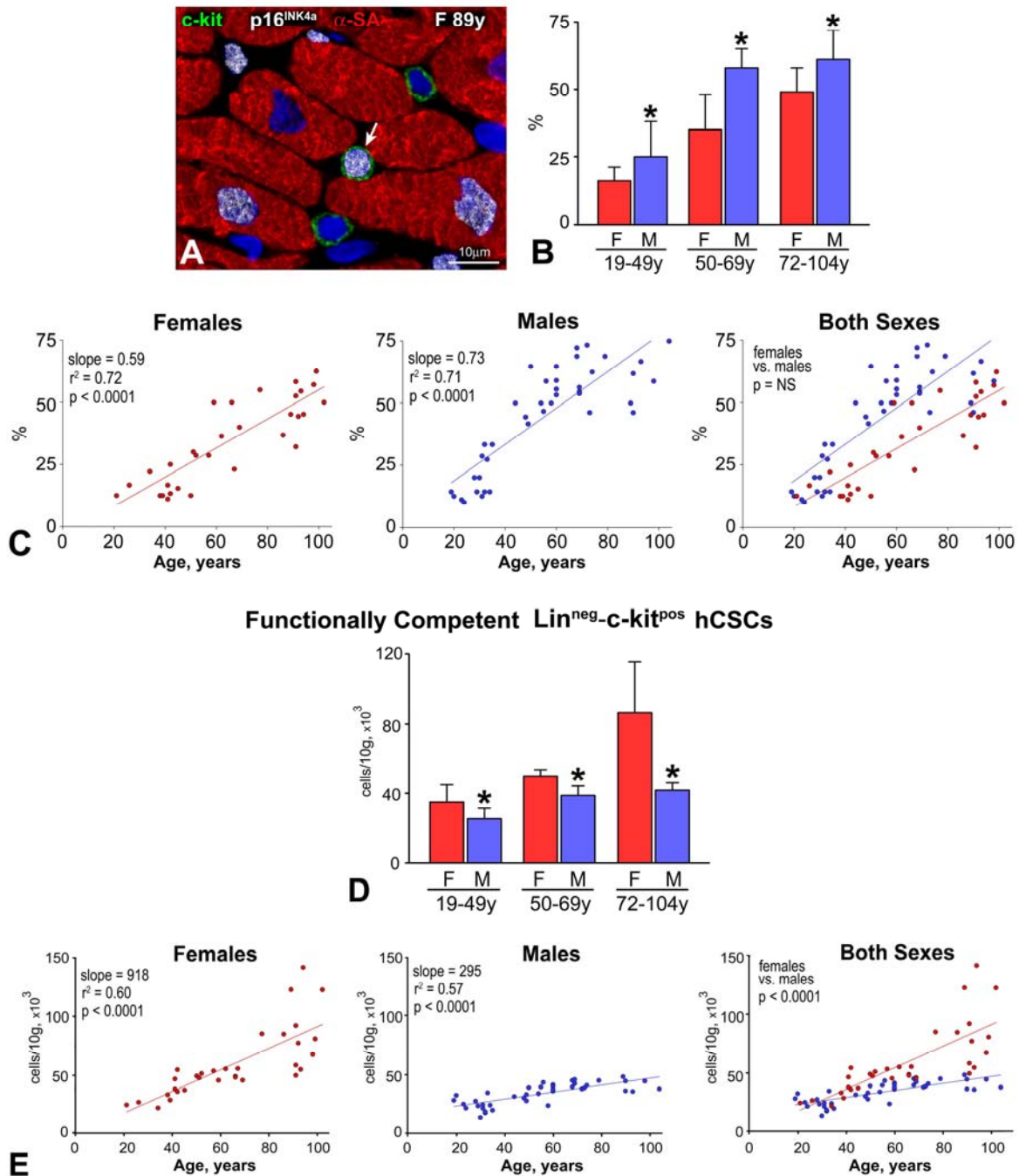


**Figure 1. Aging and myocyte senescence and death.** **A**, The fraction of p16<sup>INK4a</sup>-positive myocytes is consistently lower in women than men. **B**, The rate of increase in the fraction of p16<sup>INK4a</sup>-positive myocytes with age is lower in the female than in the male LV. **C**, The fraction of apoptotic myocytes in the LV is lower in women than men. F: female; M: male. \*p<0.05 vs. F. **D**, The rate of increase of apoptotic myocytes with age is similar in the female and male LV. **E**, At 20 years of age, the female (red) and male (blue) LV contains 4 and 6 x 10<sup>9</sup> cardiomyocytes, respectively. Curves are derived by combining the yearly levels of apoptosis shown in panel D and the prediction that cell death lasts 4 hours (see ref. 15). In the absence of cell regeneration, 5% of LV myocytes (200 x 10<sup>6</sup> in the female LV and 300 x 10<sup>6</sup> in the male LV) would be left at 63 and 48 years of age in the female and male LV, respectively.



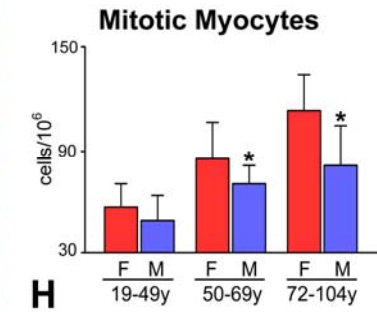
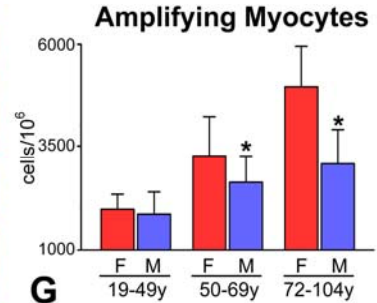
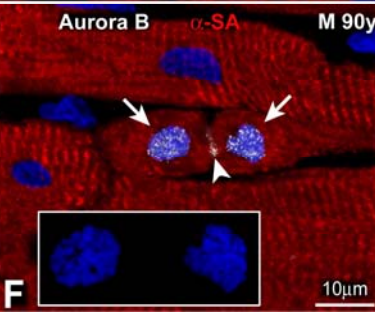
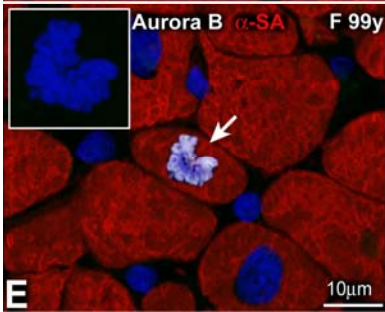
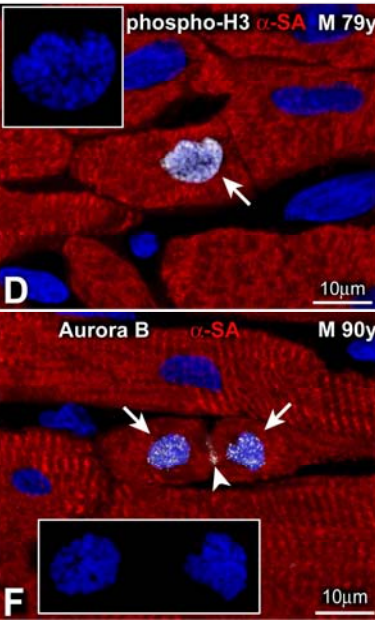
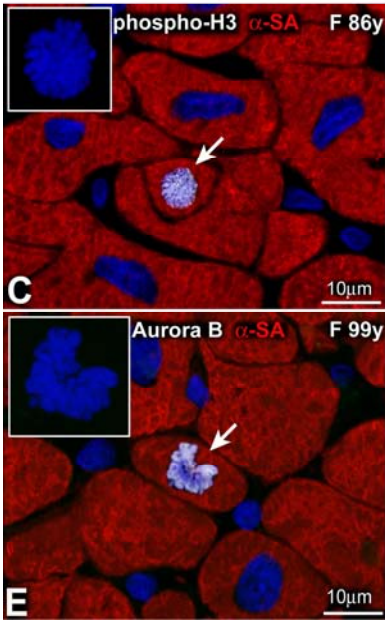
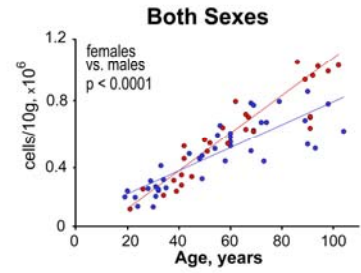
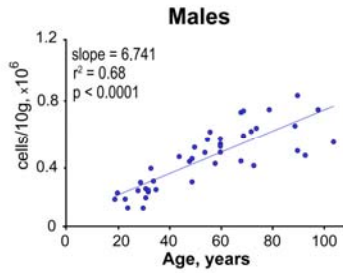
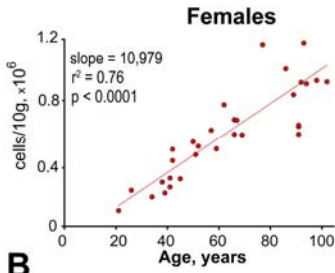
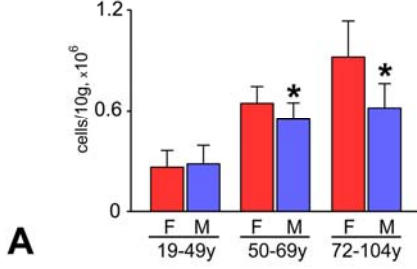
**Figure 2. Aging and hCSC growth.** **A**, The number of lineage negative (Lin<sup>neg</sup>) c-kit-positive (c-kit<sup>pos</sup>) hCSCs/10g of myocardium increases with age more in women than men. F: female; M: male. \*p<0.05 vs. F. **B**, The rate of increase of Lin<sup>neg</sup>-c-kit<sup>pos</sup> hCSCs with age is higher in the female than in the male LV. **C**, The fraction of cycling Lin<sup>neg</sup>-c-kit<sup>pos</sup> hCSCs in the LV is higher in middle-age and old women than men. F: female; M: male. \*p<0.05 vs. F. **D**, The rate of increase of cycling Lin<sup>neg</sup>-c-kit<sup>pos</sup> hCSCs with age is higher in the female than in the male LV. **E**, BrdU labeled (white) c-kit-positive (green) hCSCs at different stages of mitosis. The fraction of BrdU-labeled mitoses was plotted as a function of time (h: hours). Individual values are shown together with mean±SD.

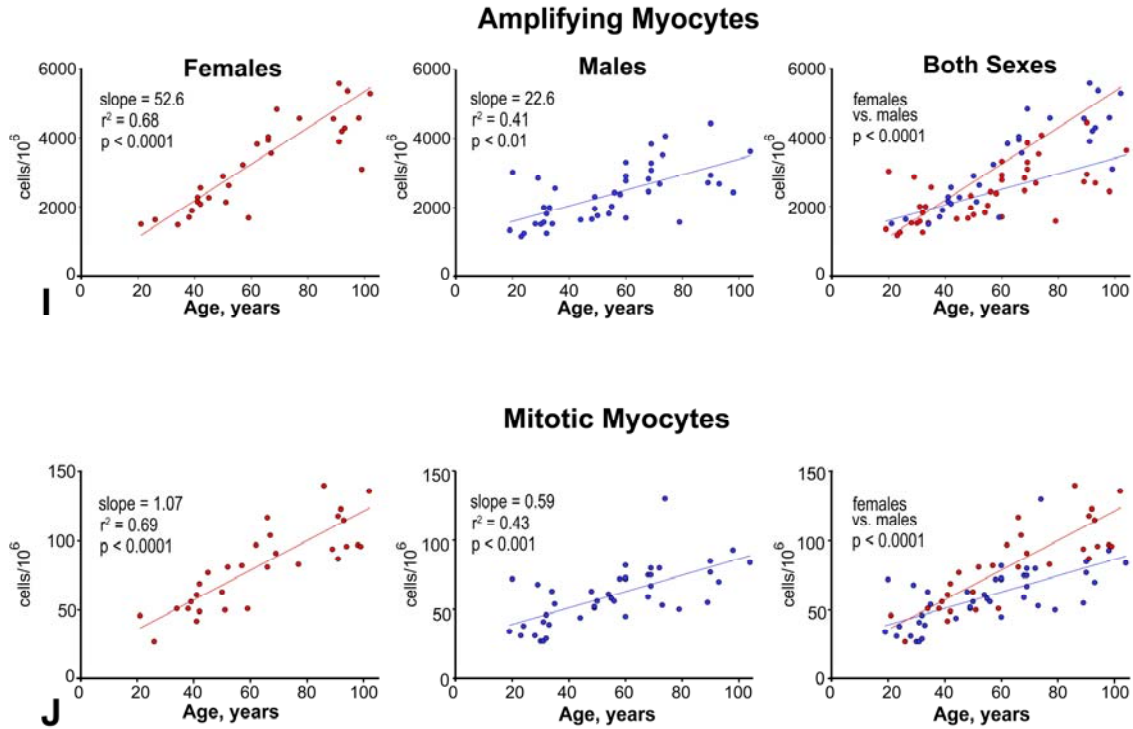
### Senescent hCSCs



**Figure 3. Aging and hCSC senescence.** **A**, Example of p16<sup>INK4a</sup>-positive hCSC (white, arrow). **B**, The fraction of p16<sup>INK4a</sup>-positive hCSCs is consistently lower in women than men. F: female; M: male. \*p<0.05 vs. F. **C**, The rate of increase in the fraction of p16<sup>INK4a</sup>-positive hCSCs with age is similar in the female and male LV. **D**, The number of functionally-competent hCSCs/10g of LV is higher in women than men at all ages. **E**, The rate of increase in the number of functionally-competent hCSCs/10g of LV with age is higher in women than men. Age and gender are indicated in panel A.

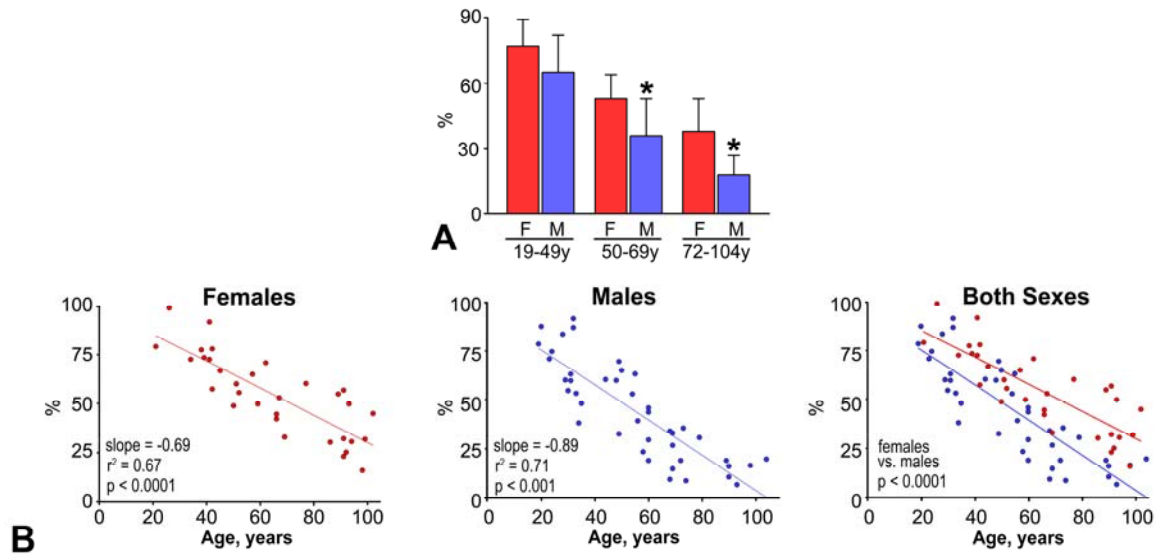
### Myocyte Progenitors and Precursors



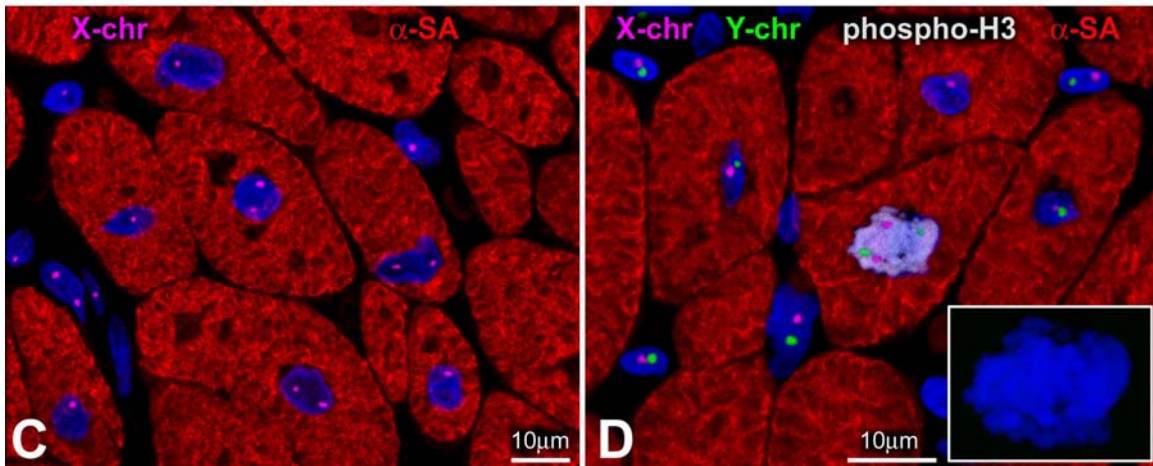
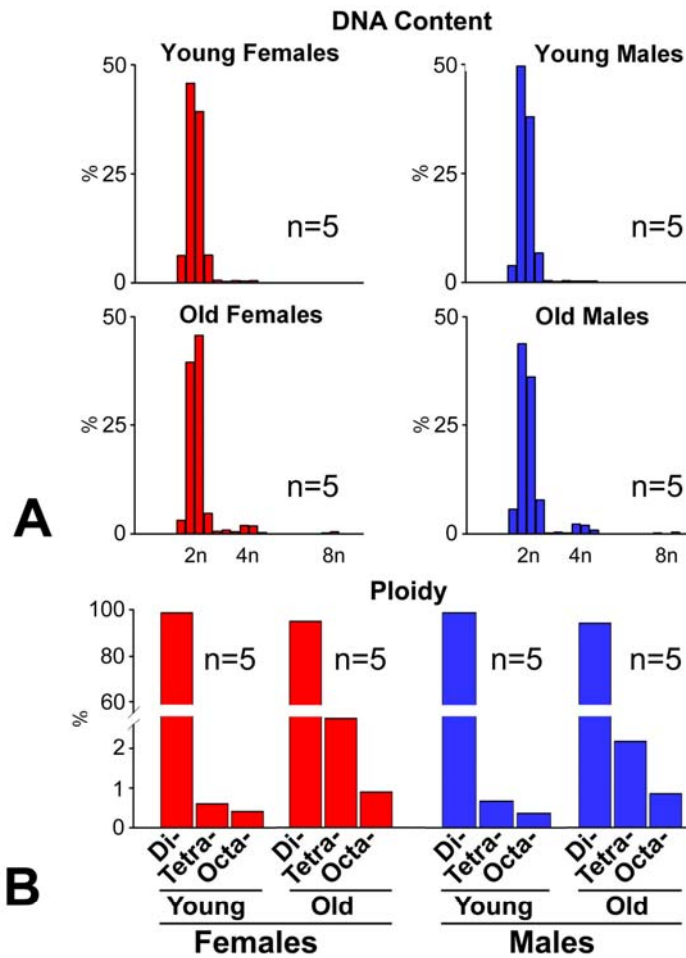


**Figure 4. Aging, myocyte progenitors and precursors, and amplifying myocytes.** **A**, The number of myocyte progenitors-precursors/10g of myocardium increases with age more in women than men. F: female; M: male. \* $p < 0.05$  vs. F. **B**, The rate of increase of myocyte progenitors-precursors with age is higher in the female than in the male LV. **C-F**, Small amplifying myocytes are positive for phospho-H3 (C and D: white, arrows) and aurora B kinase (E and F: white, arrows). In panel F, aurora B kinase is located in the two sets of telophase chromosomes and at the cleavage furrow of the dividing myocyte (arrowhead). Insets in C-F illustrate the organization of chromosomes in the dividing cells. **G** and **H**, The fraction of myocytes positive for Ki67 (G) and phospho-H3 (H) increases with age more in women than men. F: female; M: male. \* $p < 0.05$  vs. F. **I** and **J**, The rate of increase with age of amplifying myocytes positive for Ki67 (I) and mitotic myocytes positive phospho-H3 (J) is higher in the female than in the male LV.

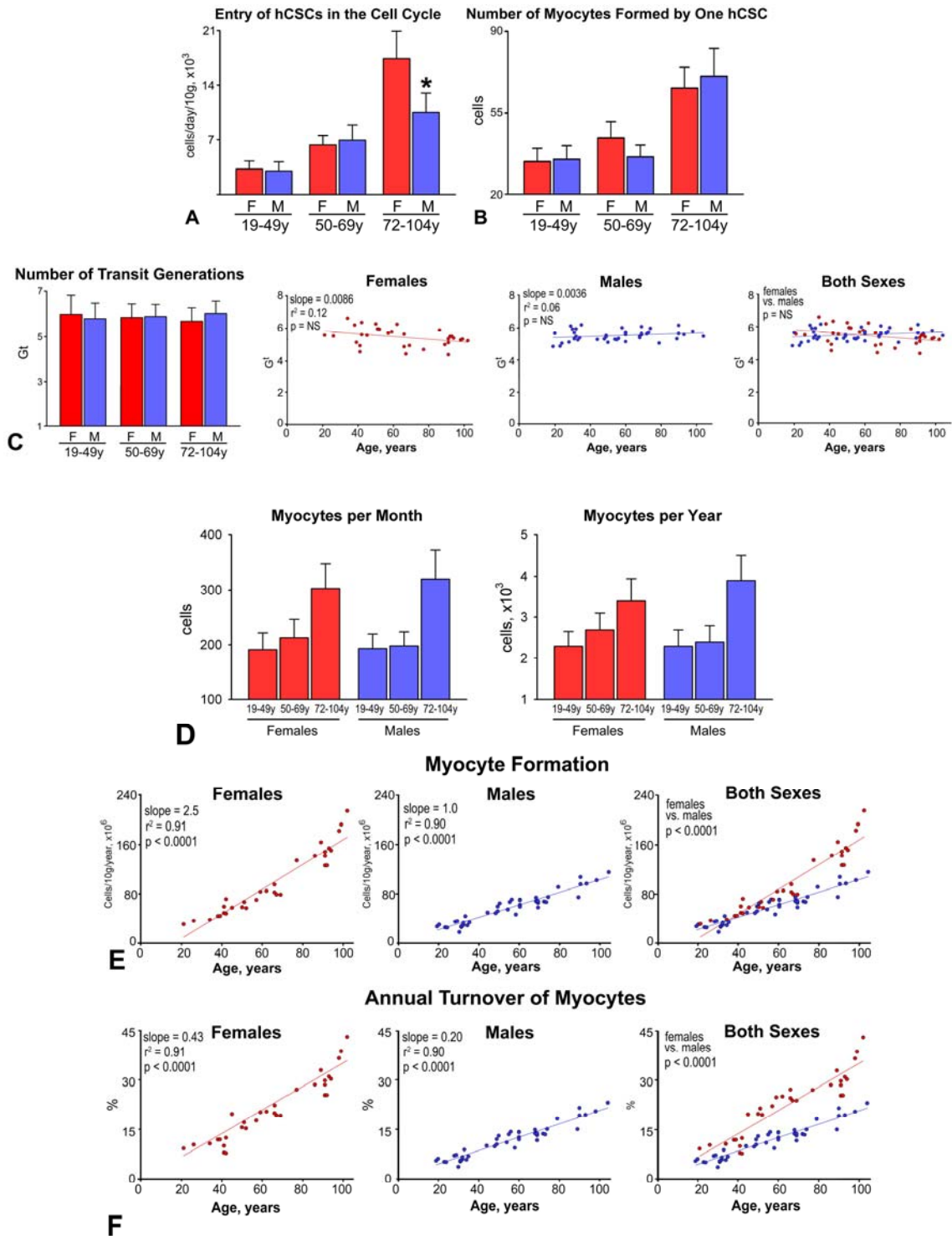
### Post-Mitotic Non-Senescent Myocytes



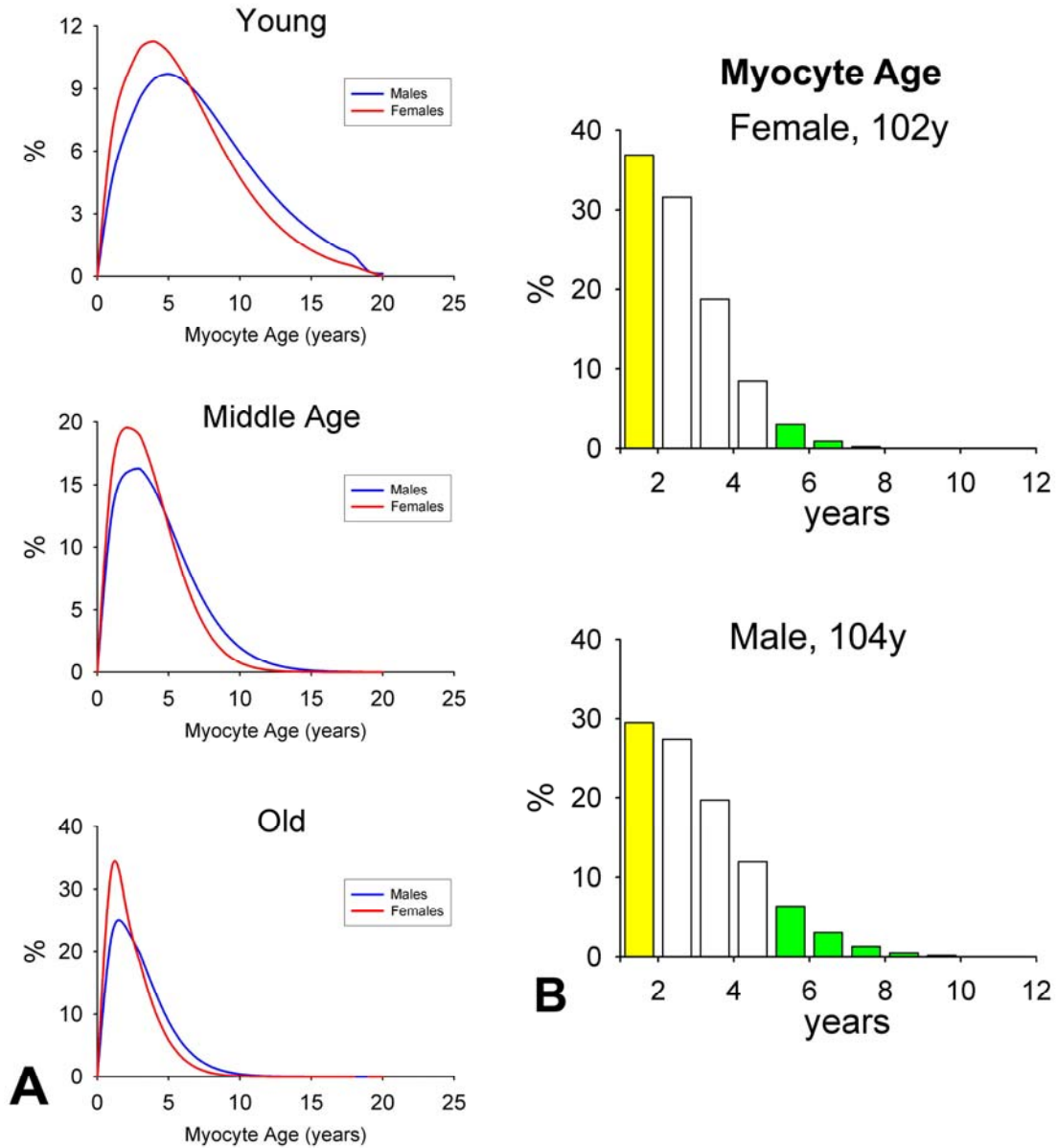
**Figure 5. Aging and post-mitotic myocytes.** **A**, The fraction of young non-dividing myocytes decreases with age less in women than men. F: female; M: male. \* $p < 0.05$  vs. F. **B**, The rate of decrease in the proportion of young non-dividing myocytes with age is lower in females than males.



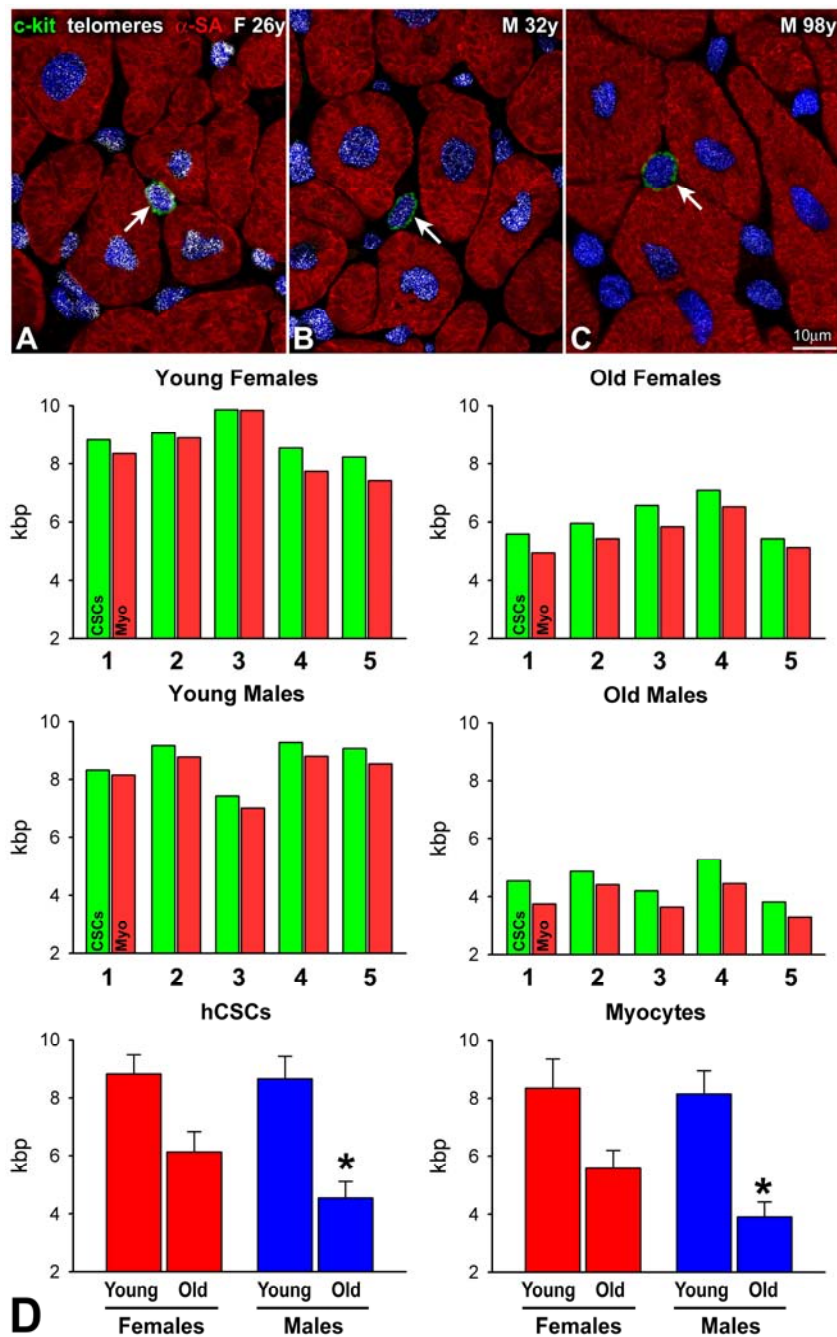
**Figure 6. Aging, ploidy and cell fusion.** **A**, Frequency distribution of DNA content in young and old female and male cardiomyocytes. **B**, Fractions of diploid, tetraploid and octaploid myocyte nuclei. **C**, Example of myocytes in a female heart; myocyte nuclei carry at most two X-chromosomes (magenta dots). **D**, Male heart in which a dividing myocyte labeled by phospho-H3 (white) shows two sets of sex chromosomes (X-chromosome, magenta; Y-chromosome, green). The inset illustrates the organization of chromosomes in the dividing cell.



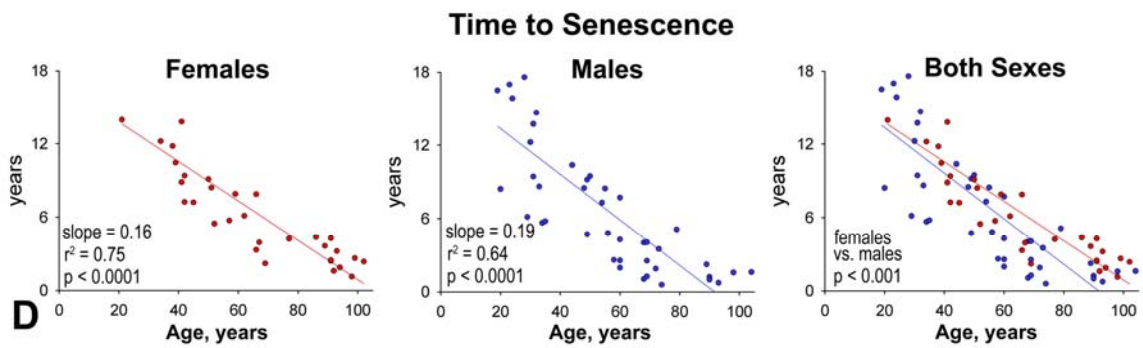
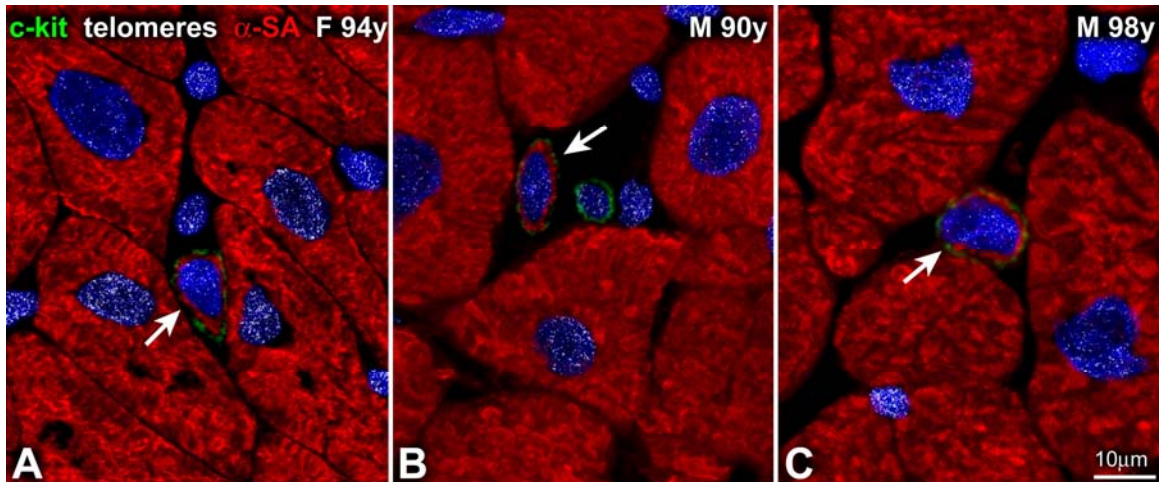
**Figure 7. Aging and myocyte formation.** **A**, Number of activated hCSCs. F: female; M: male. \* $p < 0.05$  vs. F. **B**, Myocytes generated by a single hCSC. **C**, Number of divisions experienced by hCSCs before post-mitotic myocytes are formed. **D**, Number of post-mitotic myocytes generated by a single hCSC. **E**, The rate of myocyte formation with age is higher in the female than in the male myocardium. **F**, The degree of myocyte turnover with age is higher in the female than in the male myocardium.



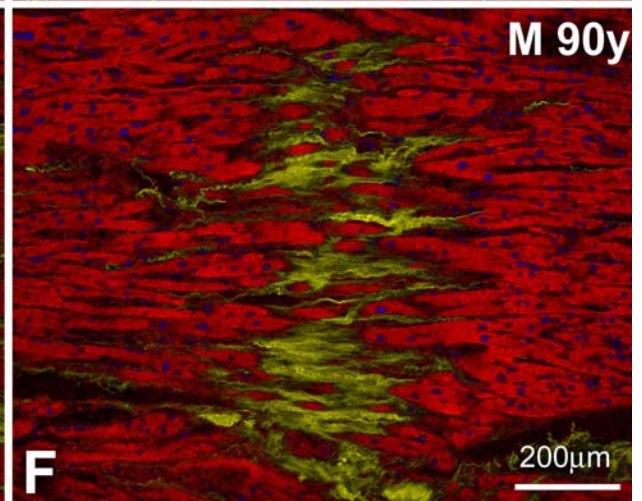
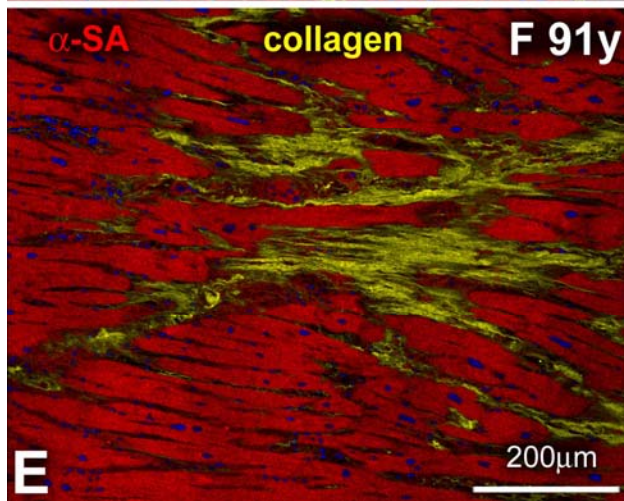
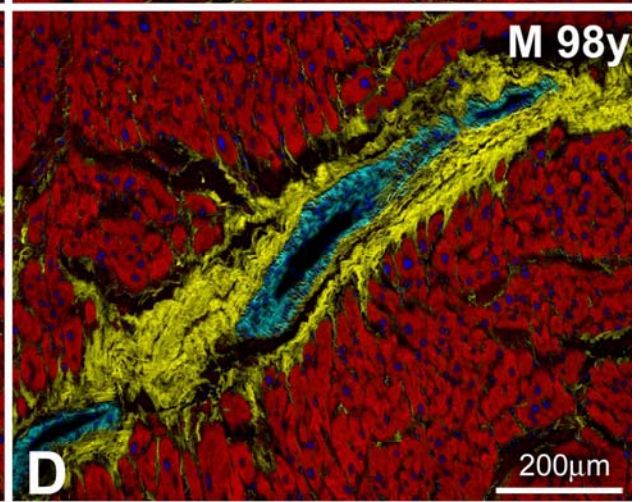
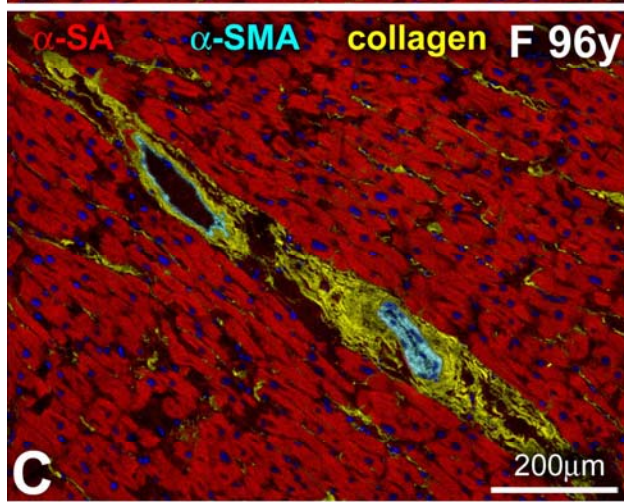
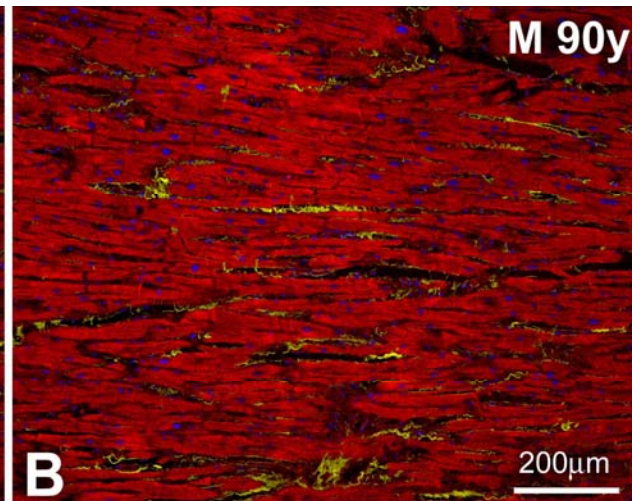
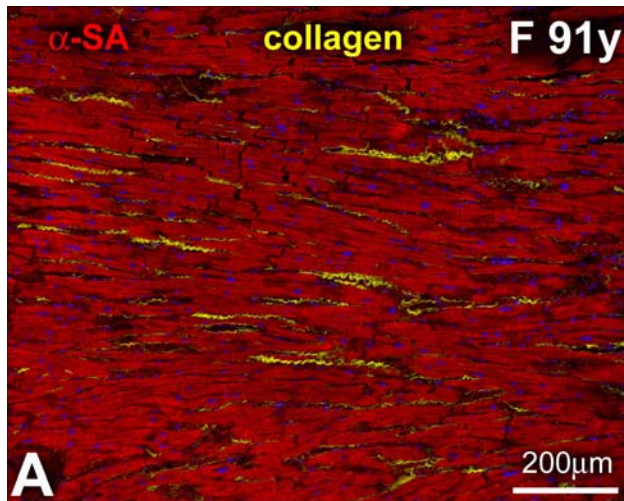
**Figure 8. Organ aging and myocyte age.** **A**, The frequency distribution of myocyte age is shifted to the right in men. **B**, Frequency distribution of myocyte age in a woman 102 years old and a man 104 years old. Yellow area: myocytes younger than 2 years. Green area: myocytes older than 5.

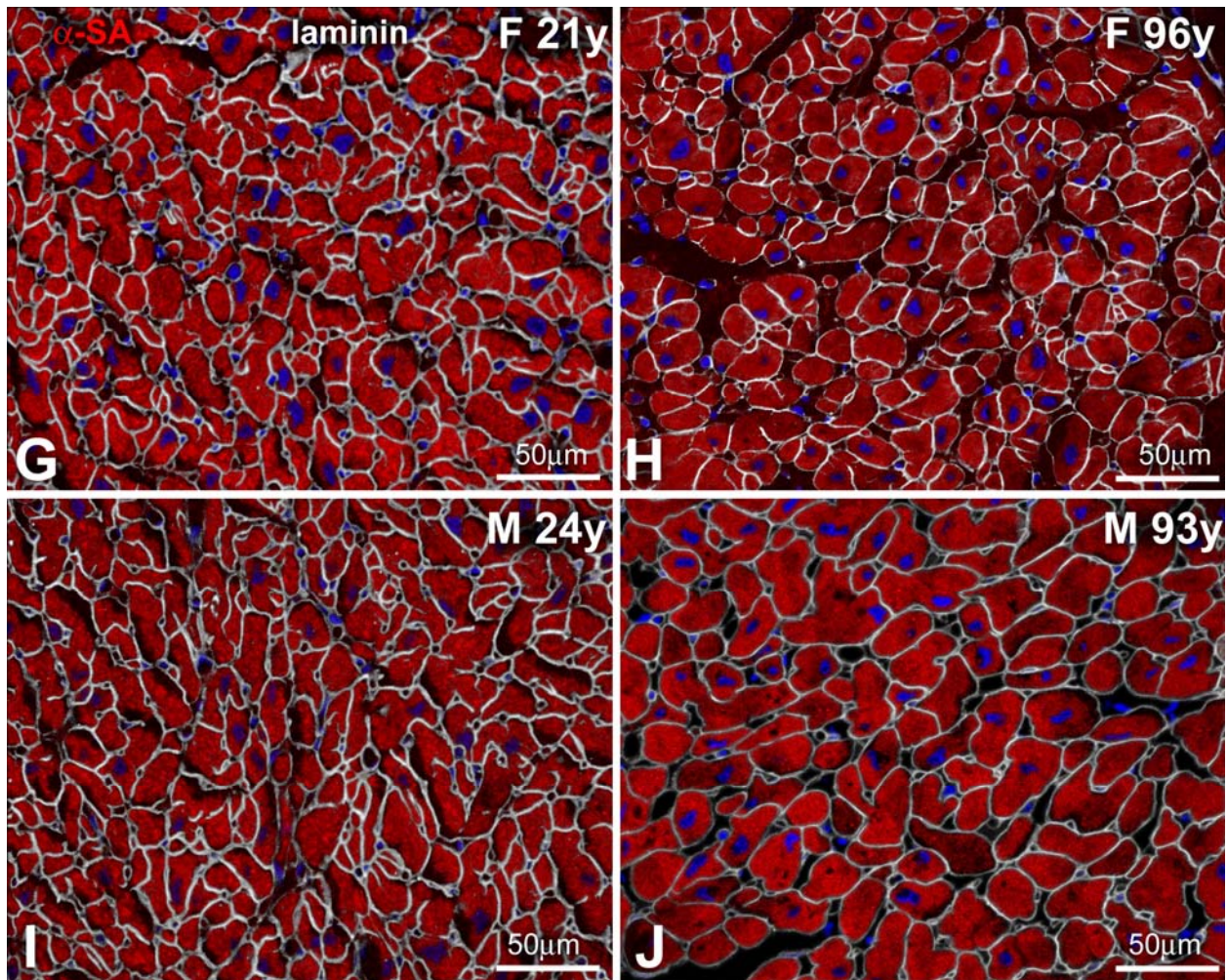


**Figure 9. Organ aging and telomere length in hCSCs and myocytes. A-C,** Detection of telomeres by Q-FISH (white dots) in c-kit-positive hCSCs (green, arrows) and cardiomyocytes in the young female (A) and in the young (B) and old (C) male heart. **D,** Telomere length in hCSCs and myocytes are shown individually and together in the four groups of hearts examined. F: female; M: male. \*p<0.05 vs. F.

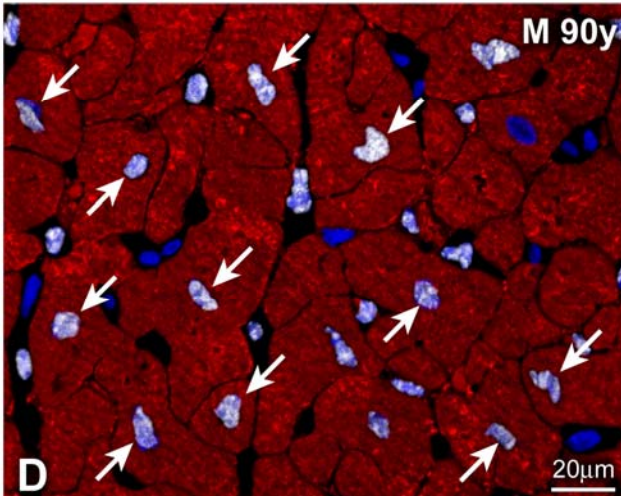
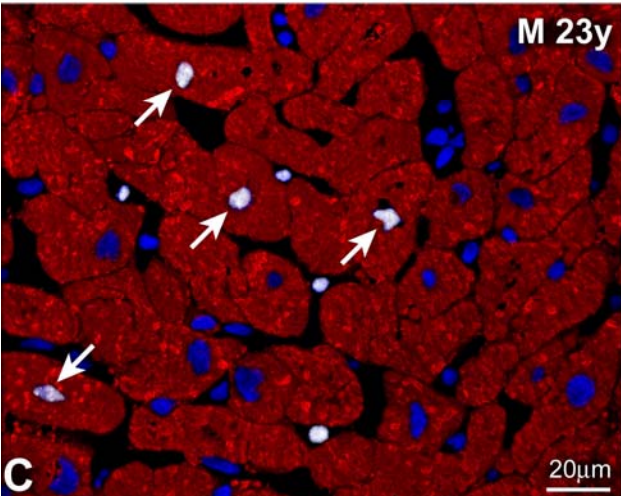
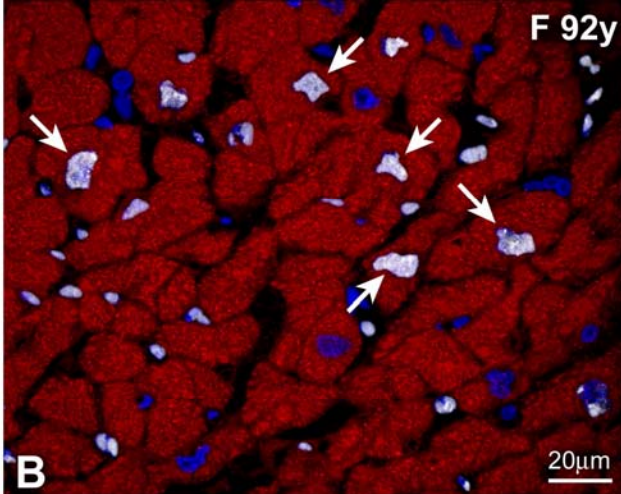
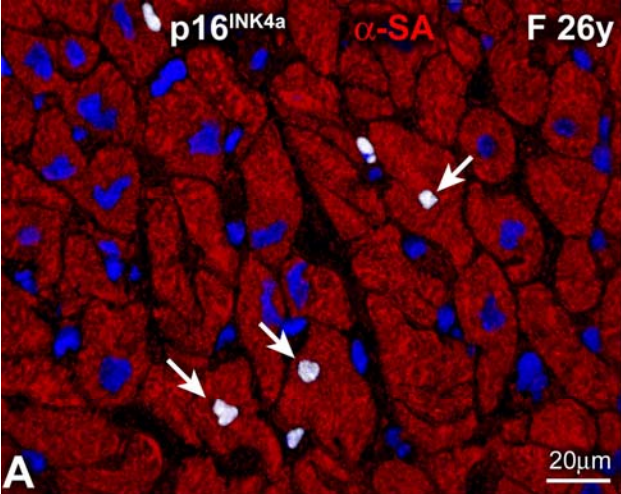


**Figure 10. Organ aging and myocyte senescence.** A-C, Myocyte precursors (c-kit, green;  $\alpha$ -SA, red) in the old female (A) and male (B and C) heart have telomeres shorter than 4kbp. D, The rate of acquisition of myocyte senescence becomes faster with age and it is slower in women than men.





**Figure I. Aging and myocardial structure.** A-F, Minimal increases in interstitial fibrosis (collagen, yellow) are present in the left ventricle (LV) of old female and male hearts (A and B). Perivascular fibrosis (C and D) and foci of reparative fibrosis (E and F) are present in old female and male LV. Coronary arterioles are defined by  $\alpha$ -smooth muscle actin ( $\alpha$ -SMA, bright blue). **G-J**, Cardiomyocytes ( $\alpha$ -sarcomeric actin:  $\alpha$ -SA, red), defined by laminin (white), are similar in cross-sectional area in young female and male hearts (G and I). The increase in myocyte size with age is less apparent in the female than in the male LV (H and J). Age and gender are indicated in each panel. F: female; M: male; y: years.



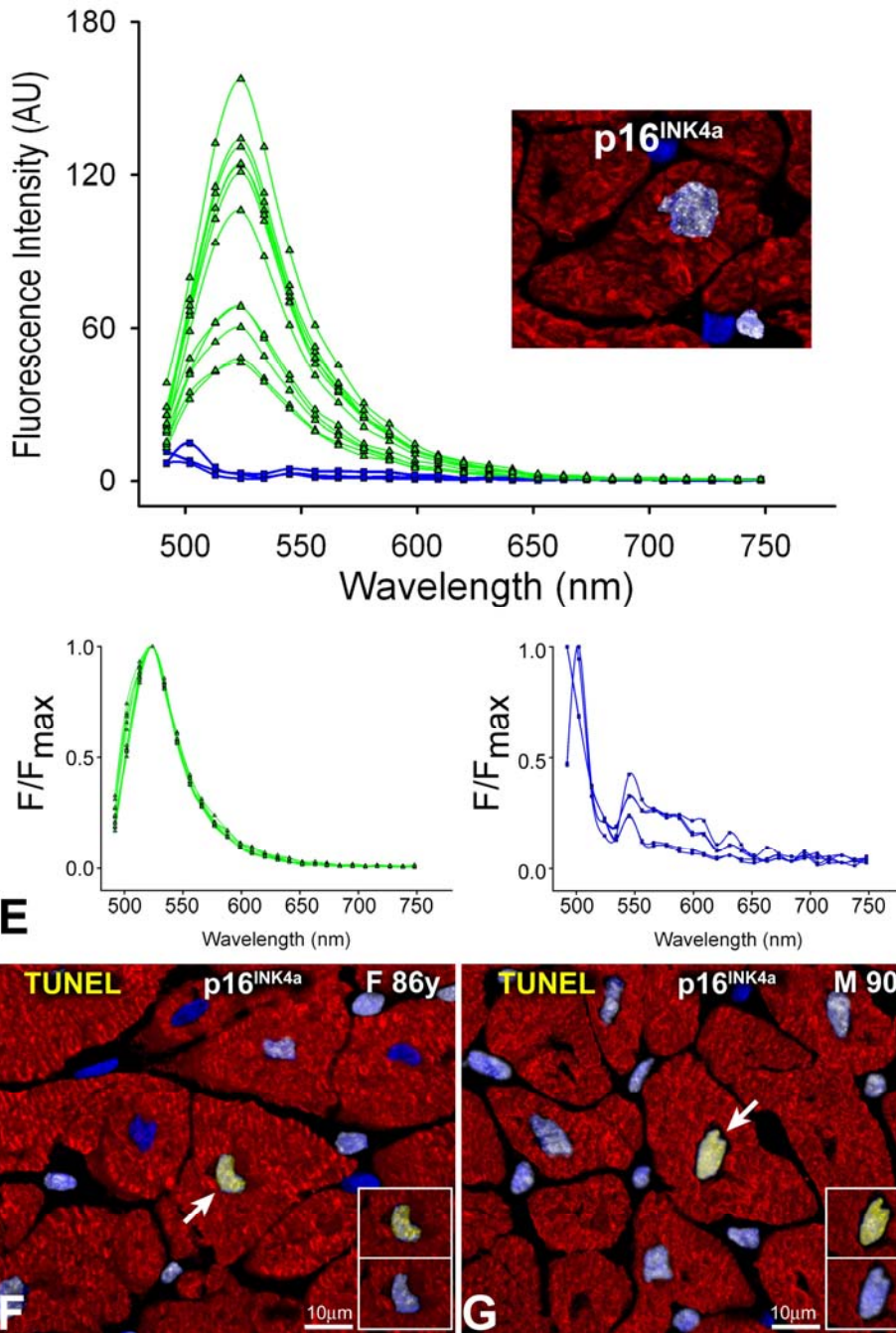


**Figure II. Myocyte senescence and apoptosis.** A-D, The presence of p16<sup>INK4a</sup> (white) in myocyte nuclei is limited in the young female and male LV (A and C; arrows) and involves a larger number of cells in the old heart of both genders (B and D). Myocytes are stained by  $\alpha$ -SA (red). E, Emission spectra of p16<sup>INK4a</sup>-positive (green lines) and p16<sup>INK4a</sup>-negative (blue lines) myocyte nuclei. Inset: example of p16<sup>INK4a</sup>-labeled nuclei used for this analysis. Following normalization for fluorescence intensity, emission spectra of p16<sup>INK4a</sup>-positive myocyte nuclei are essentially superimposable, while emission spectra for tissue autofluorescence of p16<sup>INK4a</sup>-negative myocyte nuclei have a different shape. F and G, TUNEL (yellow) and p16<sup>INK4a</sup>-positive (white) myocyte nuclei (arrows) in the female (F) and male (G) LV. Insets illustrate separately TUNEL and p16<sup>INK4a</sup> labeling.

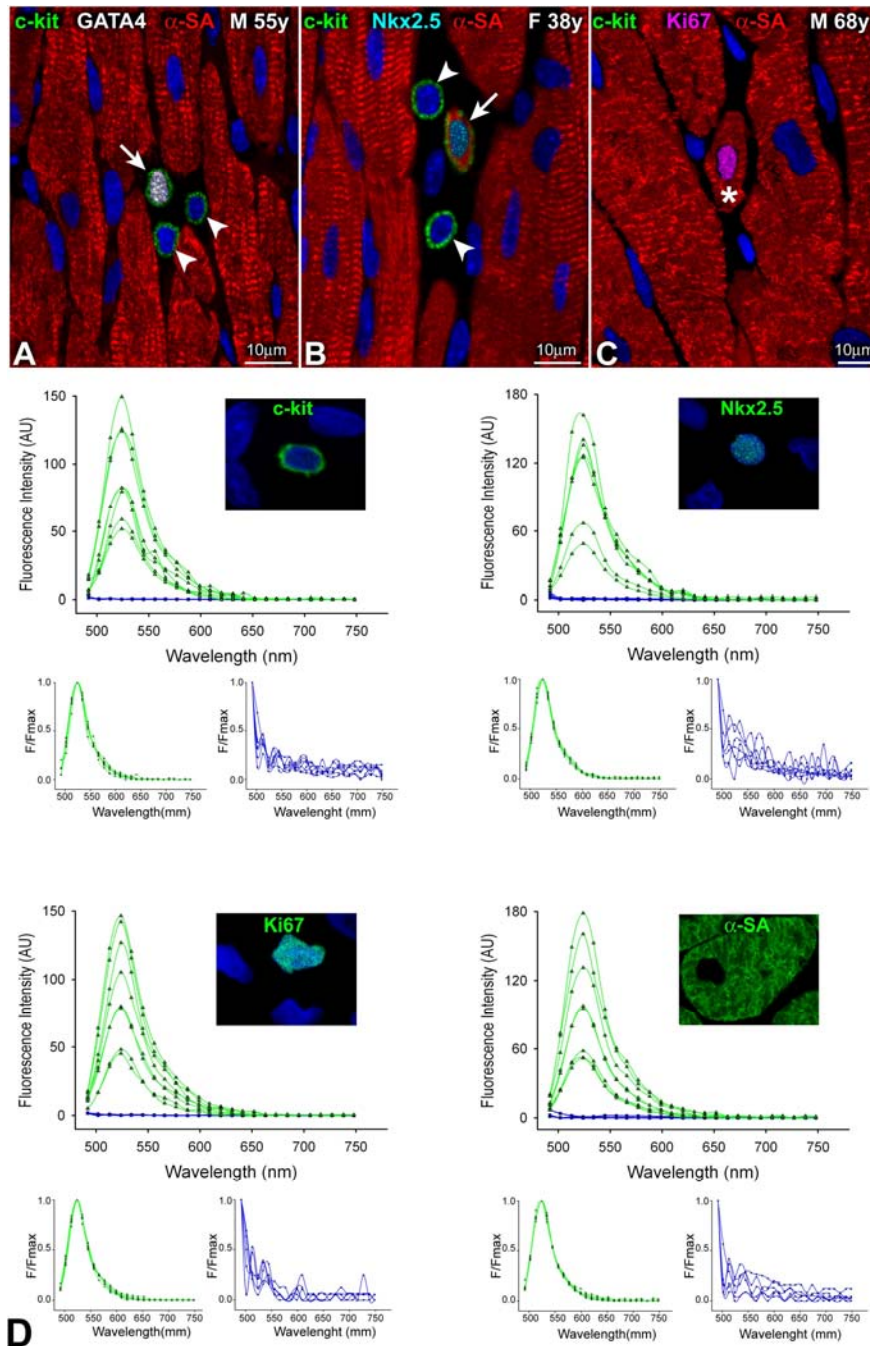


**Figure III. Myocyte progenitors and precursors.** A-C, Lineage negative hCSCs (arrowheads) are negative for transcription factors and cytoplasmic proteins (A and B). Myocyte progenitors (A, arrow) are c-kit-positive (green) and express GATA4 (white), myocyte precursors (B, arrow) are c-kit-positive and express Nkx2.5 (bright blue) and  $\alpha$ -SA (red), and amplifying myocytes (C, asterisk) are small cycling cells, positive for Ki67 (magenta) and lack c-kit. D, Emission spectra of c-kit, Nkx2.5, Ki67 and  $\alpha$ -SA positive (green lines) and negative (blue lines) cells. Examples of labeled nuclei and cells used for this analysis are shown in the insets. Following normalization for fluorescence intensity, emission spectra of c-kit, Nkx2.5, Ki67 and  $\alpha$ -SA positive cells are superimposable. The emission spectra for tissue autofluorescence have a different shape.

Figure IV

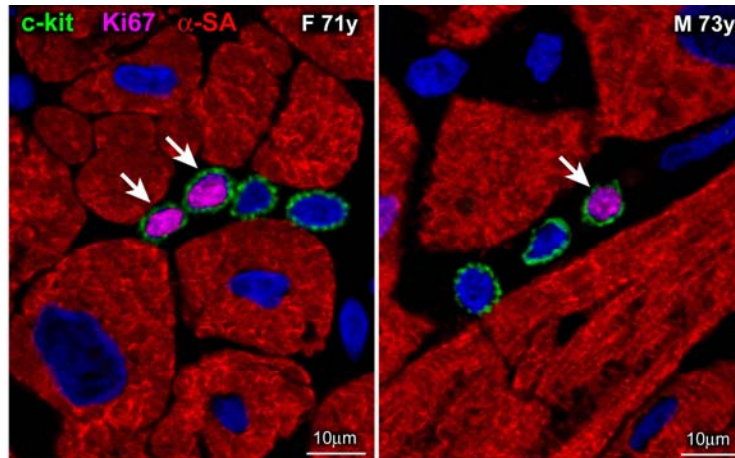


Figure V

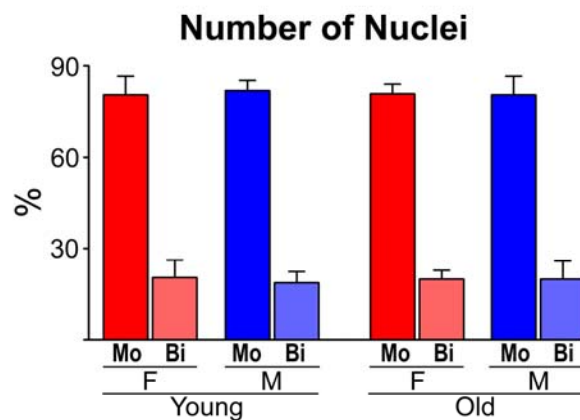
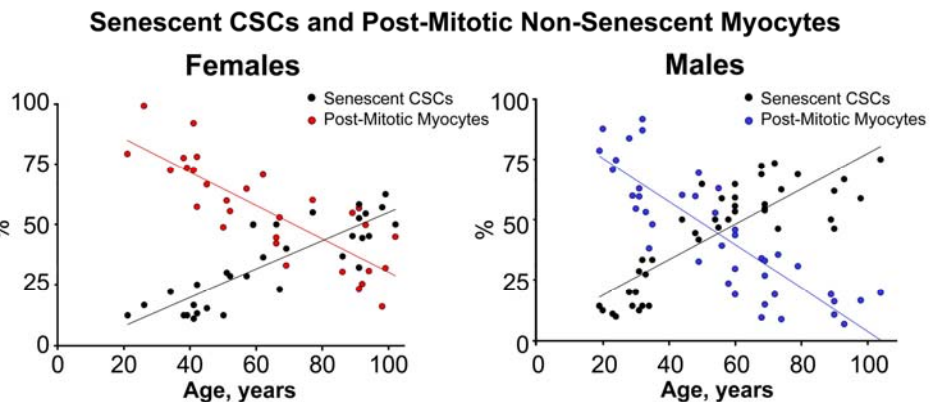


Figure VI



**Figure IV. Cycling hCSCs.** Small niches of  $\text{Lin}^{\text{neg}}\text{-c-kit}^{\text{pos}}$  hCSCs (green) containing Ki67 labeled cells (magenta, arrows).

**Figure V. Number of myocyte nuclei.** Percentage of mononucleated (Mo) and binucleated (Bi) myocytes in the young (19-49 years old) and old (72-104 years old) female and male heart.

**Figure VI. Aging and post-mitotic non-senescent and senescent myocytes.** In both women and men, the fraction of young non-dividing myocytes decreases with age, while the percentage of senescent  $\text{p16}^{\text{INK4a}}$ -positive cells increases. These data were presented separately in Figures 3C and 5B.

Figure VII

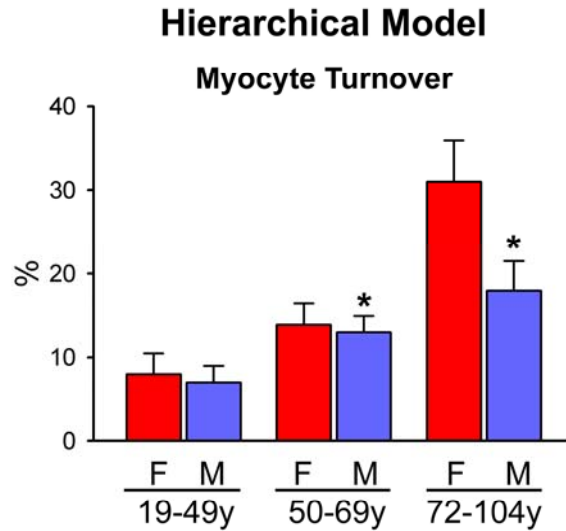


Figure VIII

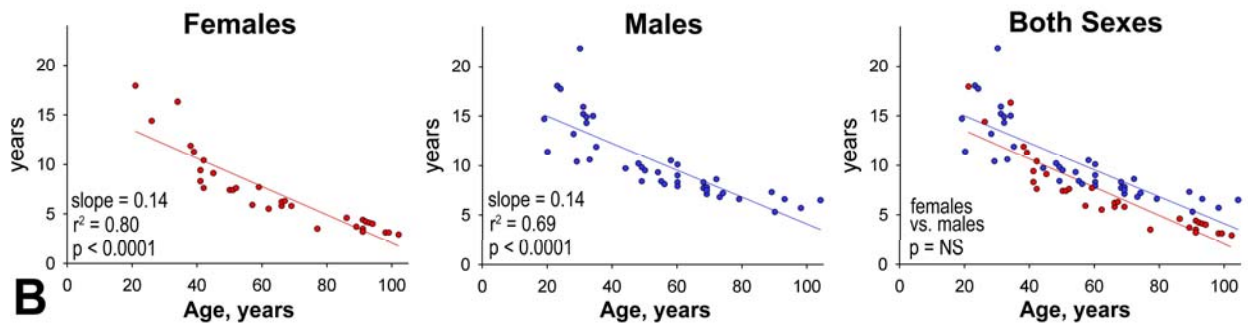
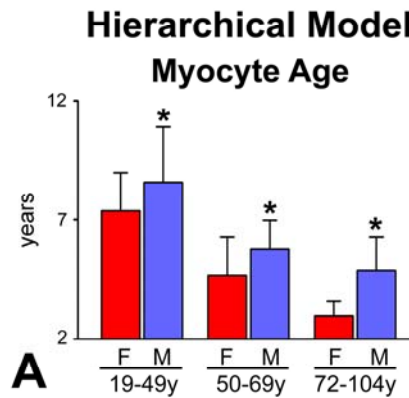
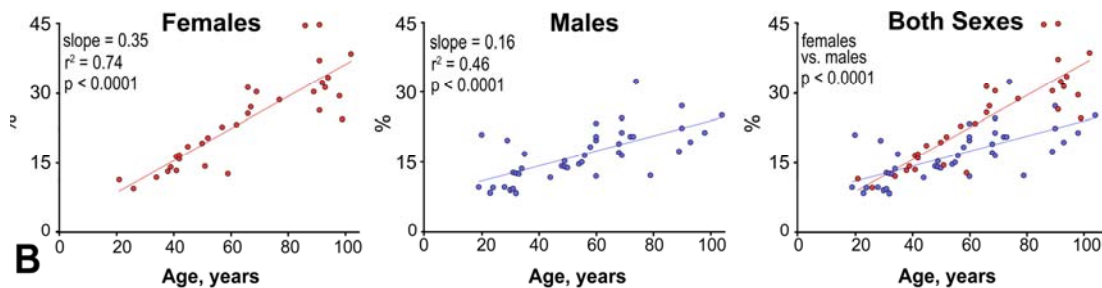
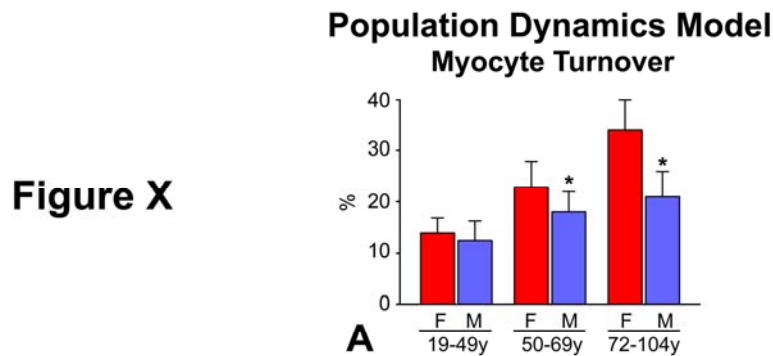
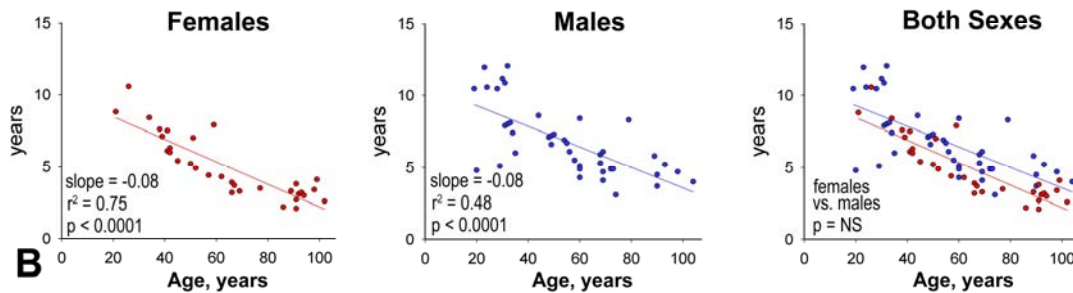
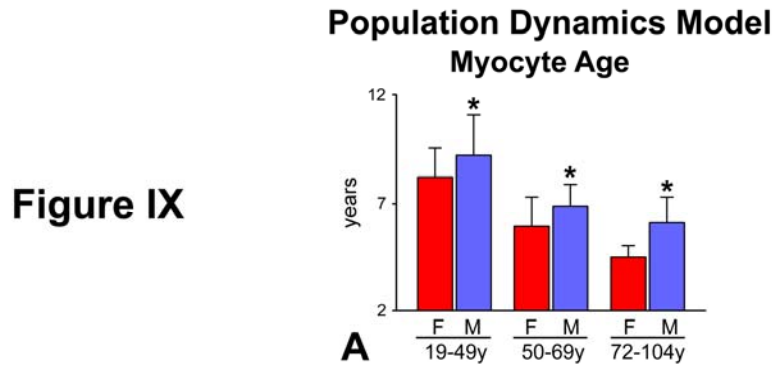


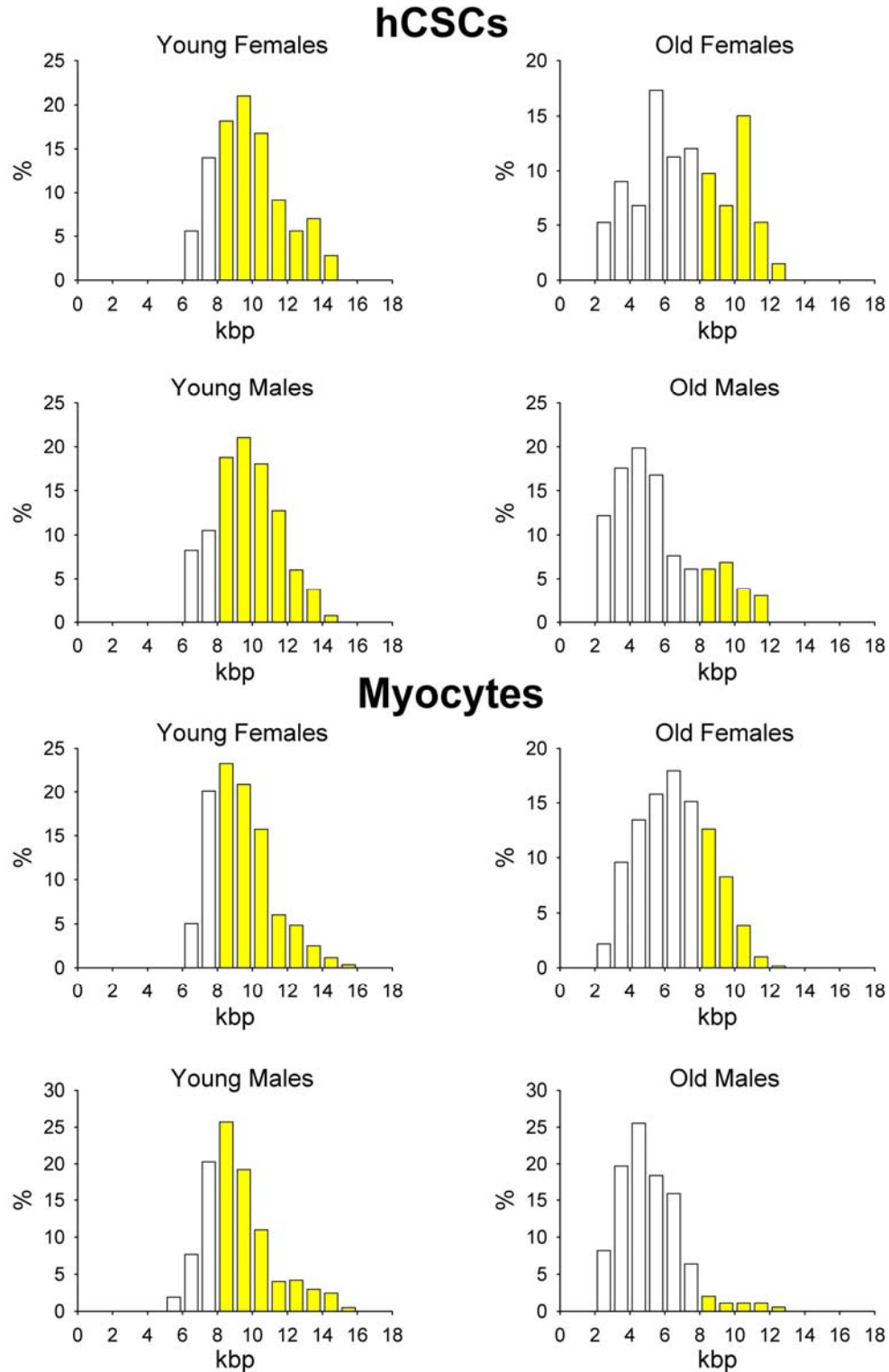
Figure VII. Aging and myocyte replacement based on the hierarchical model. Myocyte turnover is higher in middle-age and old women than men. F: female; M: male. \* $p < 0.05$  vs. F.

Figure VIII. Organ age and average myocyte age based on the hierarchical model. **A**, Younger myocytes are present in the female heart. F: female; M: male. \* $p < 0.05$  vs. F. **B**, Inverse relationship between organ and myocyte age.



**Figure IX. Organ age and average myocyte age based on population dynamics model. A,** Younger myocytes are present in the female heart. F: female; M: male. \* $p < 0.05$  vs. F. **B,** Inverse relationship between organ and myocyte age.

**Figure X. Aging and myocyte replacement based on population dynamics model. A,** Myocyte turnover is higher in middle-age and old women than men. F: female; M: male. \* $p < 0.05$  vs. F. **B,** The rate of myocyte turnover with age is higher in the female than in the male myocardium.



**Figure XI. Telomere length in hCSCs and myocytes.** Frequency distribution of telomere length in hCSCs and cardiomyocytes. Yellow area: nuclei with telomeres equal and longer than 8kbp.

## **Table I. Inclusion Criteria**

---

### **Clinical Criteria**

1. Sudden death associated with traumatic injury
2. Death within 5 days of hospitalization in the absence of cardiovascular disease
3. Absence of hypertension, diabetes or ischemic heart disease
4. Body weight within 20% of optimal weight according to sex, height and age
5. Lack of clinically recognized systemic disorders

### **Anatomical Criteria**

1. Lack of atherosclerosis of major coronary arteries or reduction of luminal diameter <30%
2. Lack of acute or healed myocardial infarction
3. Heart weight <500g
4. Absence of diffuse emphysema and chronic inflammation of the respiratory system
5. Lack of malignant neoplasm with multiple metastatic localizations

### **Histological Criteria**

1. Absence of neoplasms of the hematopoietic system
  2. Lack of amyloidosis, tuberculosis and sarcoidosis
  3. Negative for diffuse interstitial and perivascular fibrosis
  4. Lack of thickening and hyalinosis of the intermediate-sized coronary vessels
  5. Absence of foci of replacement fibrosis or presence of lesions <2 mm in diameter
  6. Lack of inflammation of the myocardial interstitium
  7. Absence of myocytolytic and contraction band necrosis
-

**Table II. Patients and Cardiac Characteristics**

| Age (years) | Gender | Body Weight (kg) | Height (cm) | Body Mass Index (kg/m <sup>2</sup> ) | Heart Weight (g) | LV Weight (g) | Cause of Death            |
|-------------|--------|------------------|-------------|--------------------------------------|------------------|---------------|---------------------------|
| 104         | M      | 70               | 170         | 24.2                                 | 265              | 195           | pneumonia                 |
| 102         | F      | 50               | 150         | 22.2                                 | 240              | 180           | cerebral aneurism         |
| 99          | F      | 45               | 145         | 21.4                                 | 187              | 139           | pulmonary thromboembolism |
| 98          | M      | 50               | 170         | 17.3                                 | 215              | 165           | gastric adenocarcinoma    |
| 98          | F      | 65               | 173         | 21.7                                 | 234              | 175           | cerebral aneurism         |
| 96          | F      | 50               | 160         | 19.6                                 | 200              | 150           | pulmonary thromboembolism |
| 94          | F      | 40               | 150         | 17.8                                 | 200              | 148           | pneumonia                 |
| 93          | M      | 75               | 175         | 24.5                                 | 325              | 250           | pulmonary thromboembolism |
| 93          | F      | 40               | 165         | 14.7                                 | 175              | 130           | intestinal occlusion      |
| 92          | F      | 52               | 152         | 21.6                                 | 201              | 150           | abdominal aorta aneurism  |
| 91          | F      | 50               | 155         | 20.8                                 | 240              | 175           | pulmonary thromboembolism |
| 91          | F      | 40               | 150         | 17.8                                 | 220              | 160           | aortic aneurism           |
| 91          | F      | 40               | 150         | 17.8                                 | 155              | 115           | pulmonary thromboembolism |
| 90          | M      | 60               | 170         | 20.8                                 | 290              | 225           | pulmonary thromboembolism |
| 90          | M      | 70               | 160         | 27.3                                 | 205              | 155           | pulmonary thromboembolism |
| 89          | M      | 60               | 180         | 18.5                                 | 350              | 245           | pneumonia                 |
| 89          | F      | 63               | 165         | 23.3                                 | 200              | 148           | cerebral aneurism         |
| 86          | F      | 70               | 160         | 27.3                                 | 340              | 255           | pneumonia                 |
| 79          | M      | 66               | 164         | 24.5                                 | 194              | 151           | aortic aneurism           |
| 77          | F      | 62               | 155         | 25.8                                 | 174              | 135           | pneumonia                 |
| 75          | F      | 60               | 153         | 25.6                                 | 166              | 129           | pneumonia                 |
| 74          | M      | 65               | 165         | 23.9                                 | 247              | 192           | pulmonary thromboembolism |
| 74          | M      | 65               | 165         | 23.9                                 | 290              | 220           | pneumonia                 |
| 74          | F      | 72               | 174         | 23.8                                 | 267              | 204           | cerebral aneurism         |
| 73          | M      | 67               | 168         | 23.7                                 | 236              | 174           | cerebral aneurism         |
| 72          | M      | 70               | 168         | 24.8                                 | 212              | 156           | pneumonia                 |
| 71          | F      | 64               | 165         | 23.5                                 | 188              | 138           | acute trauma              |

|    |   |    |     |      |     |     |                              |
|----|---|----|-----|------|-----|-----|------------------------------|
| 69 | M | 85 | 185 | 24.8 | 230 | 175 | pulmonary embolism           |
| 69 | M | 55 | 165 | 22.9 | 250 | 210 | pneumonia                    |
| 69 | M | 60 | 170 | 20.8 | 240 | 180 | pneumonia                    |
| 69 | F | 70 | 170 | 24.2 | 215 | 165 | pulmonary artery embolism    |
| 68 | M | 50 | 165 | 18.4 | 240 | 180 | acute distress resp. syndrom |
| 68 | M | 62 | 160 | 24.2 | 243 | 189 | pneumonia                    |
| 67 | F | 65 | 170 | 22.5 | 240 | 180 | pneumonia                    |
| 66 | F | 55 | 165 | 20.2 | 315 | 240 | abdominal aortic aneurism    |
| 66 | F | 70 | 160 | 27.3 | 280 | 210 | aortic dissection            |
| 62 | F | 67 | 155 | 27.9 | 270 | 210 | pneumonia                    |
| 60 | M | 70 | 185 | 20.5 | 290 | 230 | pneumonia                    |
| 60 | M | 60 | 175 | 19.6 | 180 | 140 | pneumonia                    |
| 60 | M | 75 | 180 | 23.1 | 355 | 280 | pneumonia                    |
| 60 | M | 50 | 160 | 19.5 | 255 | 190 | gastrointestinal hemorrhage  |
| 60 | F | 53 | 158 | 21.2 | 178 | 131 | acute trauma                 |
| 59 | F | 55 | 175 | 18.0 | 225 | 170 | pneumonia                    |
| 58 | M | 60 | 160 | 23.4 | 330 | 270 | pneumonia                    |
| 57 | F | 80 | 170 | 27.7 | 310 | 240 | acute hemorrh. pancreatitis  |
| 56 | M | 85 | 186 | 24.6 | 240 | 180 | pneumonia                    |
| 55 | M | 76 | 170 | 26.3 | 180 | 135 | pneumonia                    |
| 54 | M | 85 | 175 | 27.8 | 200 | 150 | pneumonia                    |
| 52 | F | 55 | 155 | 22.9 | 174 | 140 | acute hemorrhage             |
| 51 | F | 62 | 163 | 23.3 | 250 | 184 | pneumonia                    |
| 50 | M | 70 | 185 | 20.5 | 230 | 180 | pneumonia                    |
| 50 | F | 76 | 165 | 27.9 | 185 | 150 | hemorrhagic ictus            |
| 49 | M | 70 | 169 | 24.5 | 210 | 160 | cerebral stroke              |
| 49 | M | 73 | 174 | 24.1 | 219 | 169 | suicide                      |
| 48 | M | 68 | 175 | 22.2 | 310 | 235 | pneumonia                    |
| 45 | F | 58 | 156 | 23.8 | 161 | 124 | acute trauma                 |
| 44 | M | 70 | 180 | 21.6 | 175 | 130 | aortic rupture               |
| 42 | F | 59 | 165 | 21.7 | 170 | 130 | abdominal aortic aneurism    |
| 42 | F | 53 | 160 | 20.7 | 170 | 115 | pneumonia                    |
| 41 | F | 40 | 130 | 23.7 | 190 | 140 | multiorgan failure           |
| 41 | F | 63 | 165 | 23.1 | 180 | 140 | cerebral aneurism            |

|    |   |     |     |      |     |     |                             |
|----|---|-----|-----|------|-----|-----|-----------------------------|
| 39 | F | 63  | 176 | 20.3 | 220 | 174 | cerebral aneurism           |
| 38 | F | 52  | 160 | 20.3 | 250 | 210 | acute trauma                |
| 35 | M | 75  | 188 | 21.2 | 261 | 201 | acute trauma                |
| 34 | M | 90  | 180 | 27.8 | 275 | 206 | gastrointestinal hemorrhage |
| 34 | F | 63  | 158 | 25.2 | 205 | 158 | pneumonia                   |
| 33 | M | 90  | 180 | 27.8 | 270 | 215 | craniopharyngioma           |
| 32 | M | 75  | 180 | 23.1 | 194 | 143 | acute trauma                |
| 32 | M | 70  | 175 | 22.9 | 215 | 160 | suicide                     |
| 31 | M | 75  | 165 | 27.5 | 280 | 205 | acute trauma                |
| 31 | M | 80  | 170 | 27.7 | 320 | 240 | abdominal aortic aneurism   |
| 30 | M | 65  | 177 | 20.7 | 200 | 150 | suicide                     |
| 29 | M | 80  | 187 | 22.9 | 215 | 160 | acute trauma                |
| 28 | M | 100 | 190 | 27.7 | 360 | 210 | thoracic aortic aneurism    |
| 26 | F | 53  | 158 | 21.2 | 192 | 142 | pneumonia                   |
| 24 | M | 70  | 177 | 22.3 | 270 | 200 | acute trauma                |
| 23 | M | 80  | 195 | 21.0 | 390 | 300 | acute trauma                |
| 21 | F | 50  | 165 | 18.4 | 210 | 170 | acute trauma                |
| 20 | M | 81  | 183 | 24.2 | 193 | 149 | acute trauma                |
| 19 | M | 70  | 185 | 20.5 | 340 | 300 | cerebral aneurism           |

---

Heart weight was determined following removal of epicardial fat.

**Table III.** Magnitude of Sampling

| Parameter                                      | Aggregate sample size    | Sample size (mean $\pm$ SD) | Sampling Error |
|--|--------------------------|-----------------------------|----------------|
| p16 <sup>INK4a</sup> -positive Myocytes        |                          |                             |                |
| Females  | 8,817 <sup>(1)</sup>     | 275 $\pm$ 99                | 6.0%           |
| Males  | 10,785 <sup>(1)</sup>    | 257 $\pm$ 128               | 6.2%           |
| Apoptotic Myocytes                             |                          |                             |                |
| Females  | 2,449,600 <sup>(1)</sup> | 76,550 $\pm$ 35,064         | 6.3%           |
| Males  | 2,883,825 <sup>(1)</sup> | 68,663 $\pm$ 27,781         | 5.8%           |
| Lin <sup>neg</sup> -c-kit <sup>pos</sup> hCSCs |                          |                             |                |
| Females  | 8,267 <sup>(2)</sup>     | 258 $\pm$ 84                | 4.4%           |
| Males  | 12,349 <sup>(2)</sup>    | 294 $\pm$ 97                | 4.3%           |
| Proliferating hCSCs                            |                          |                             |                |
| Females  | 994 <sup>(1)</sup>       | 31.1 $\pm$ 7.8              | 3.2%           |
| Males  | 1,143 <sup>(1)</sup>     | 27.2 $\pm$ 6.8              | 3.0%           |
| Senescent hCSCs                                |                          |                             |                |
| Females  | 9,409 <sup>(1)</sup>     | 294 $\pm$ 128               | 1.0%           |
| Males  | 9,957 <sup>(1)</sup>     | 237 $\pm$ 74                | 1.0%           |
| Myocyte Progenitors and Precursors             |                          |                             |                |
| Females  | 8,895 <sup>(1)</sup>     | 278 $\pm$ 121               | 1.0%           |
| Males  | 9,402 <sup>(1)</sup>     | 224 $\pm$ 70                | 1.0%           |
| Amplifying Myocytes                            |                          |                             |                |
| Females  | 1,380,225 <sup>(1)</sup> | 34,500 $\pm$ 6,517          | 0.5%           |
| Males  | 1,449,000 <sup>(1)</sup> | 32,863 $\pm$ 7,215          | 0.5%           |
| Mitotic Myocytes                               |                          |                             |                |
| Females  | 2,706,900 <sup>(1)</sup> | 64,450 $\pm$ 9,947          | 0.4%           |
| Males  | 3,037,020 <sup>(1)</sup> | 72,310 $\pm$ 10,691         | 0.4%           |
| DNA Content in Myocytes                        |                          |                             |                |
| Females  | 2,035 <sup>(1)</sup>     | 204 $\pm$ 9                 | 6.9%           |
| Males  | 2,089 <sup>(1)</sup>     | 209 $\pm$ 10                | 7.0%           |
| Number of Nuclei in Myocytes                   |                          |                             |                |
| Females  | 4,441 <sup>(1)</sup>     | 444 $\pm$ 42                | 4.7%           |
| Males  | 4,384 <sup>(1)</sup>     | 438 $\pm$ 28                | 4.8%           |
| FISH for Sex Chromosomes in Myocytes           |                          |                             |                |
| Females  | 3,418 <sup>(1)</sup>     | 342 $\pm$ 53                | 5.4%           |
| Males  | 3,261 <sup>(1)</sup>     | 326 $\pm$ 60                | 5.5%           |

|                             |                      |        |      |
|-----------------------------|----------------------|--------|------|
| Telomere Length in CSCs     |                      |        |      |
| Females                     | 264 <sup>(1)</sup>   | 26±3   | 6.2% |
| Males                       | 276 <sup>(1)</sup>   | 28±3   | 6.0% |
| Telomere Length in Myocytes |                      |        |      |
| Females                     | 1,192 <sup>(1)</sup> | 119±8  | 2.9% |
| Males                       | 1,120 <sup>(1)</sup> | 112±12 | 3.0% |

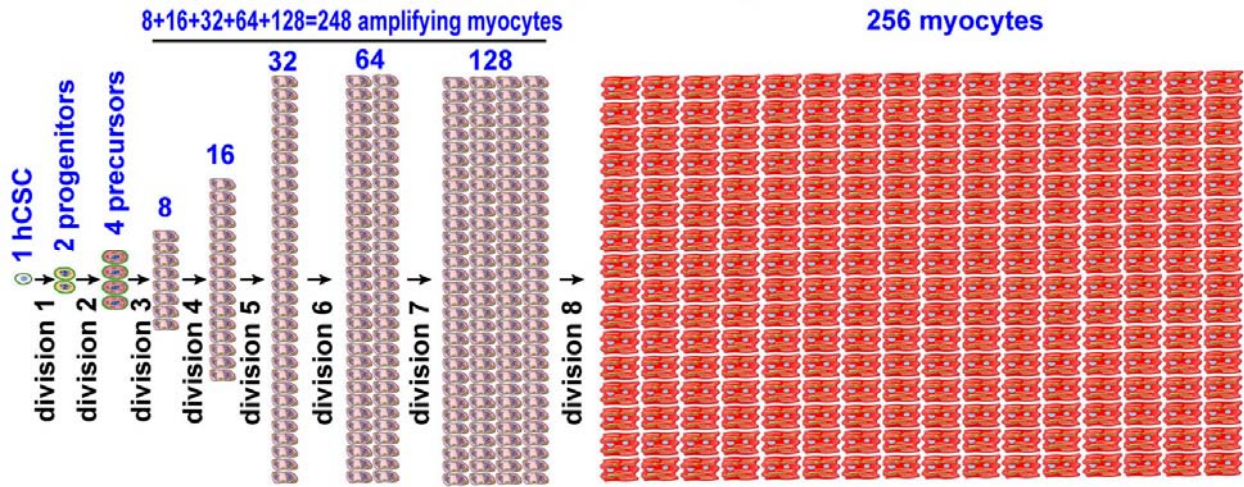
---

<sup>(1)</sup> Total number of nuclei analyzed; <sup>(2)</sup> Area of myocardium analyzed to establish the number of Lin<sup>neg</sup>-c-kit<sup>pos</sup> hCSCs.

**Table IV.** Immunolabeling

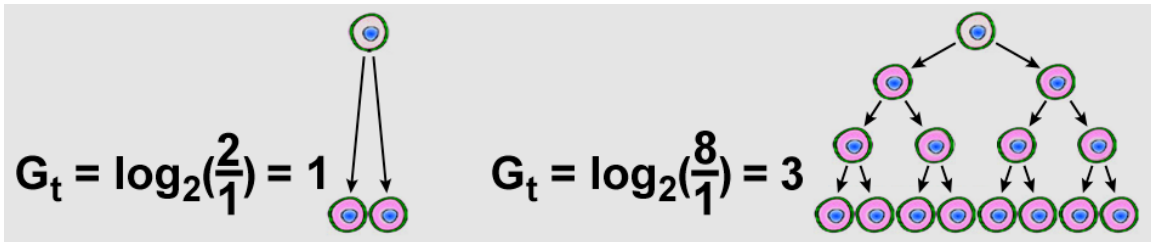
| Protein                    | Antibody          | Labeling            | Fluorochromes    |
|----------------------------|-------------------|---------------------|------------------|
| c-kit                      | rabbit polyclonal | direct and indirect | F, T, QD655      |
| GATA4                      | rabbit polyclonal | indirect            | T, Cy5           |
| Nkx2.5                     | goat polyclonal   | indirect            | F, T, Cy5        |
| $\alpha$ -sarcomeric actin | mouse monoclonal  | direct              | F, T, Cy5, QD655 |
| $\alpha$ -smooth actin     | mouse monoclonal  | direct              | T, Cy5, QD655    |
| Ki67                       | rabbit polyclonal | indirect            | F, T, Cy5        |
| Phospho-H3                 | mouse monoclonal  | direct, indirect    | T, Cy5, QD655    |
| Aurora B kinase            | rabbit polyclonal | indirect            | T, Cy5           |
| p16 <sup>INK4a</sup>       | goat polyclonal   | indirect            | F, T, Cy5        |
| Nuclear DNA                | DAPI, PI          | N/A                 | N/A              |
| X and Y chromosomes        | DNA probe         | direct              | F, Cy3           |
| TUNEL                      | TdT/dUTP          | direct              | F, T             |

Direct labeling: primary antibody conjugated with the fluorochrome. Indirect labeling: species-specific secondary antibody conjugated with the fluorochrome. F: fluorescein isothiocyanate, T: tetramethyl rhodamine isothiocyanate, Cy3: cyanine 3, Cy5: cyanine 5, QD655: quantum dots with emission at 655 nm.



**Scheme I. Exponential Cell Growth**

This scheme shows that division of one hCSC may lead to the formation of 256 myocytes by 8 consecutive divisions. The first gives rise to 2 progenitors, the second to 4 precursors and the third to 8 amplifying myocytes; if these cells divide 5 times, 256 mature myocytes are formed.



**Scheme II. Transit Generations of hCSCs**

G<sub>t</sub> reflects the number of divisions that 1 hCSC goes through before differentiation is acquired. For example, with 1 transit generation (1 G<sub>t</sub>), 2 mature cells are formed and with 3 G<sub>t</sub>, 8 mature cells are created.